# NASA TECHNICAL MEMORANDUM

NASA TM X- 72653

COPY NO.



(NASA-TM-X-72653) VERIFICATION OF A LANDING DYNAMICS COMPUTER PROGRAM USING VIKING LANDER DATA (NASA) 63 p HC $4.25 CSCL 22B

N75-20447

Unclas
G3/18 14763

# VERIFICATION OF A LANDING DYNAMICS COMPUTER PROGRAM USING VIKING LANDER DATA

By

Ralph J. Muraca
Langley Research Center
Hampton, Virginia

C. Anderson King
Hampton Technical Center
LTV Aerospace Corporation
Hampton, Virginia

April 7, 1975

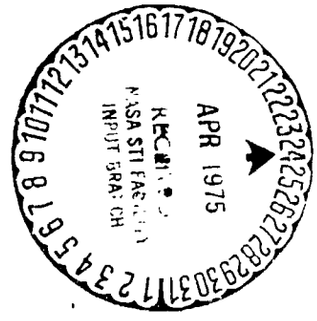




NATIONAL AERONAUTICS AND SPACE ADMINISTRATION
LANGLEY RESEARCH CENTER, HAMPTON, VIRGINIA 23665

| 1. Report No. | 2. Government Accession No. | 3. Recipient's Catalog No. |
|---|---|---|
| 72653 | | |

| 4. Title and Subtitle | 5. Report Date |
|---|---|
| Verification of a Landing Dynamics Computer Program Using Viking Lander Data | April 7, 1975 |
| | 6. Performing Organization Code |

| 7. Author(s) | 8. Performing Organization Report No. |
|---|---|
| Dr. Ralph J. Muraca<br>Mr. C. Anderson King | |
| | 10. Work Unit No. |

| 9. Performing Organization Name and Address | | 11. Contract or Grant No. |
|---|---|---|
| NASA<br>Langley Research Center<br>Hampton, VA 23665 | Hampton Technical Center<br>LTV Aerospace Corporation<br>Hampton, VA 23665 | |
| | | 13. Type of Report and Period Covered |
| 12. Sponsoring Agency Name and Address | | TM X |
| NASA | | 14. Sponsoring Agency Code |

15. Supplementary Notes

Interim fechnical information release subject to possible revision and/or later formal publication.

16. Abstract

An investigation was conducted to verify the accuracy of the Landing Dynamics Computer Program (LDCP) used to simulate the landing event of the Viking Lander (VL) onto the Martian surface. This verification was achieved by comparing the analytical data with results from a test program involving a dynamically scaled model of a VL configuration. A secondary objective of this study was to evaluate the sensitivity of the VL to initial rates and orientations, configuration modifications, and footpad friction.

| 17. Key Words (Suggested by Author(s)) (STAR category underlined) | 18. Distribution Statement |
|---|---|
| Landing Dynamics, Planetary Soft Lander Data, Three Leg Planetary Lander Data, Comparison with Lander Test Data | Unclassified - Unlimited |

| 19. Security Classif. (of this report) | 20. Security Classif. (of this page) | 21. No. of Pages | 22. Price* |
|---|---|---|---|
| Unclassified | Unclassified | 29 | $4.25 |

*Available from { The National Technical Information Service, Springfield, Virginia 22151
STIF/NASA Scientific and Technical Information Facility, P.O. Box 33, College Park, MD 20740

NATIONAL AERONAUTICS AND SPACE ADMINISTRATION

# VERIFICATION OF A LANDING DYNAMICS COMPUTER PROGRAM USING VIKING LANDER DATA

By Ralph J. Muraca and C. Anderson King
Langley Research Center
Hampton, Virginia

## SUMMARY

An investigation was conducted to verify the accuracy of the Landing Dynamics Computer Program (LDCP) used to simulate the landing event of the Viking Lander (VL) onto the Martian surface. This verification was achieved by comparing the analytical data with results from a test program involving a dynamically scaled model of a VL configuration. A secondary objective of this study was to evaluate the sensitivity of the VL to initial rates and orientations, configuration modifications, and footpad friction.

## INTRODUCTION

To evaluate the performance of the VL during the landing event, an analytical investigation was conducted using a Monte Carlo simulation (reference 1). The landing dynamics model used to simulate the landing event was the Landing Dynamics Computer Program (LDCP) described in the Appendix of reference 1. In the LDCP, the lander is assumed to have a

rigid body with three massless legs attached. The LDCP simulates the lander's dynamic behavior by considering the rigid body as having 6 degrees of freedom and numerically integrating the respective equations of motion.

The purpose of this paper is to verify the accuracy of the LDCP using the results of the 3/8 scale VL model drop test program (reference 2). Eighteen model landings that covered a wide variety of landing conditions and exercised the capabilities of the analysis to the fullest have been selected for comparison purposes. Included in this set are landings which exercised the three primary strut load/stroke options. Also included are landings on different types of surfaces so the effects of friction can be examined. Two landings having spikes for footpads are included to evaluate the effects of infinite friction.

Figure 1 shows a schematic of the VL configuration with only the center body, legs, and footpads. Each leg consists of three struts in an inverted tripod arrangement with a footpad attached at the junction of the struts. The primary strut contains an energy absorbtion/load limiting system composed of crushable honeycomb cartridges. Each secondary strut is attached to a load limiter which in turn is bolted to the body. The function of the load limiter is to limit the magnitude of the forces which can be transmitted to the lander body.

During the design process of the VL, the operation of the primary strut shock absorber was found to have a major effect on the lander stability. The primary strut design uses a piston-cylinder arrangement with the crushable honeycomb located in the cylinder. The force-stroke optional capabilities are within the basic design as shown in figure 2. These three strut configurations are considered in the analysis and a description of the operation of each follows.

(1) Full Deadband Strut. Before the strut can go into tension, it re-extends to its initial length. Hence, there exists a region, called the deadband, where the strut has no load carrying capability. Once it has completely re-extended, it then deforms elastically under a tension load.

(2) Bonded Honeycomb Strut. The crushable honeycomb is bonded to the strut. This results in a limited tensile load carrying capability for the strut until the honeycomb fails in tension. Once this capability is exceeded, the strut acts similar to the full deadband strut.

(3) Ratchet Strut. The cylinder is equipped with a ratchet. The strut experiences a limited deadband before the ratchet engages in its nearest slot. Once engaged, the strut then deforms elastically under a tension load.

In comparing test data with computer results, certain assumptions in the analysis preclude exact correlation. Some of the more important assumptions involved structural dynamics of the lander center body,

constancy of friction coefficient during contact between the lander's footpad and the surface, and the manner in which loads are transmitted from the surface to the lander body. Consequently, no attempt has been made to vary the initial conditions at impact to bring about a better correlation in the data.

## SYMBOLS

| | |
|---|---|
| $I_{xx}$, $I_{yy}$, $I_{zz}$ | principal moments of inertia about the body axis |
| t | time |
| $V_h$ | horizontal velocity of lander |
| $V_v$ | vertical velocity of lander |
| 1P, 1R, 1L | strut identification symbols |
| 2P, 2R, 2L | 1, 2, 3 indicates leg number |
| 3P, 3R, 3L | P is primary strut |
| | R is right secondary strut |
| | L is left secondary strut |
| $\alpha$ | landing surface slope |
| $\mu$ | coefficient of friction between footpad and landing surface |
| $\psi$, $\theta$, $\phi$ | roll, pitch, yaw angles |

## PROCEDURES

A detailed presentation of the test set up, vehicle reference axis and orientation, vehicle characteristics, and initial conditions is presented in reference 2. A summary of the initial landing conditions

for the eighteen drop cases is shown in Table 1. The definitions of the initial conditions are defined in figure 3. The direction of the slope for all landings is along the +y-axis. The direction of the horizontal velocity is defined as being positive, (called "uphill" velocity), if directed toward the landing surface, and negative, (called "downhill" velocity), if directed away from the landing surface. No cross-slope horizontal velocity existed; i.e., horizontal velocities are either uphill, downhill, or zero. In all cases, the nominal initial conditions measured from the experiment are used in the analysis, including the coefficient of friction between the footpad and the landing surface.

The time history relationships of the strut forces, the primary strut stroke lengths and the body coordinates of the center of gravity acceleration are presented for all eighteen cases (figures 4 through 39). These time histories are converted from the 3/8 scale model quantities to the full scale values for both the analysis and test. For all cases, the solid curves represent computed quantities and broken curves test quantities. In the strut force time histories, the force sign convention is positive for tension and negative for compression. The three components of the center of gravity acceleration are plotted in earth's g units. In the analysis, the normal component of acceleration during free flight is 1 g, whereas in the test no accelerations are recorded. Therefore, there exists a differential of 1 g between analysis and test normal accelerations. However, for

the comparison of the overall performance of the lander, this differential is negligible in comparing the timing and peak accelerations. The quantities that are used in the stroke length plots are basically the same for both the test and analysis. However, the quantity that is plotted from the test is the differential strut length between the actual and initial strut lengths; therefore, as the strut re-extends in the deadband region, the differential length decreases. The quantity plotted from the analysis is the maximum stroke length that the strut has experienced, therefore, when the strut re-extends, this quantity remains constant. This difference accounts for the difference between analytical and test stroke lengths which appear during certain landings. However, when the maximum stroke lengths from test and from analysis are compared, the agreement is good.

Drop Cases 1, 2, 3, 4, 5, 8, and 9 primarily demonstrate the capability of the analysis to predict the behavior of the lander. A second objective of these landings is to demonstrate the sensitivity of lander performance to attitude (roll, pitch, and yaw), horizontal velocity, and the friction coefficient between footpads and landing surface. The remaining eleven landings, Drop Cases 6, 7, 10, 11, 12, 13, 14, 15, 16, 17, and 18 are intended to evaluate the landing stability. The two objectives of this test program will be discussed separately: first, the verification of the analysis, and second, the performance sensitivity of the lander model. Table 2 shows the basic

initial conditions for each landing, the stability of the lander for these tests (if either stable or unstable) and the analysis prediction of the slopes on which the lander would be stable and unstable.

## VERIFICATION OF ANALYSIS

### General Discussion

In all cases, the analysis is in qualitative agreement with the test results. That is, the nature (tension or compression) of the secondary strut loads consistently agree with experiment for all legs at each leg contact. The sequence of leg impacts and time intervals between leg impacts are in general agreement, even in the case where one leg makes more than one contact with the landing surface. The center of gravity accelerations and the stroking length of the main struts agree well with experiment. From a quantitative viewpoint, the agreements between test and analysis are not as consistently good. In some instances, the causes of disagreement can be deduced whereas in others they remain elusive. A detailed discussion of the major discrepancies between experiment and analysis constitute the bulk of this comparison.

Five cases, Drop Cases 5, 7, 13, 15, and 17, are discussed in depth. The comparison between analysis and test results for the other thirteen cases are basically the same as for these five cases. The time histories of the remaining thirteen cases are presented in figures 14 through 39 for completeness.

## Drop Case 5

Drop Case 5 is an asymmetric landing. The lander is rolled so that the legs impact at different times (a 1-1-1 landing). In this case, the impact sequence is leg 2, leg 3, and finally leg 1. The comparison of the landing sequence and impact timing, shown on figures 4 and 5, for all three legs is good. The only large discrepancy is in the time of the second impact of leg 2. However, the lander has lost most of its kinetic energy by this time, and no noticeable effects are observed in the center of gravity acceleration.

The strut forces for all three legs show good agreement except that in the analysis the primary struts remain loaded whereas the actual struts began unloading for all three legs. The analysis predicted that leg 3 primary strut would reach the third force level; however, test results indicated only the second level is reached. This disagreement can possibly be attributed to the friction coefficient between the landing surface and the pad. At the point where the test strut began unloading, the pad's tangential force overcomes the frictional force causing the pad to begin sliding. During this time, the analytical friction force continues to be greater than its tangential force resulting in the pad remaining stationary. The variation of friction coefficient under transient conditions is very difficult to predict, consequently, no attempt has been made to include this variation in the model. Possibly, by varying the friction coefficient, the analysis will better predict the unloading behavior of the struts. However, the overall agreement in the lander's behavior is very good using the nominal value of friction.

The normal component of the acceleration at the center of gravity is in good agreement. The analysis does not predict the peak accelerations in the longitudinal and transverse directions that are experienced during the experiment.

The primary strut stroke comparisons show that legs 2 and 3 are in very good agreement with the analysis predicting only slightly more stroking than experiment. Leg 1 stroking is predicted to be much greater than actually observed due to the behavior of the primary struts as previously discussed.

## Drop Case 7

The configuration of the 3/8 scale model was modified for Drop Case 7 by installing spikes on footpads to simulate landing on a surface that produced an infinite coefficient of friction between the footpads and the surface, e.g., a footpad impacted in a hole, or against a rock.

The strut force time histories, figure 6, shows that the sequence and timing of impacts of the analysis agreed with the test. In both the analysis and the test, leg 1 impacts a second time before the lander turns over. The strut forces for all three legs are in good agreement. The primary struts reach higher load levels in the analysis than in the test. In this landing, the deadband characteristics of the primary struts are demonstrated. The primary struts of legs 2 and 3 unload and go into the deadband region while the secondary struts continue to load. Both the analysis and the test demonstrate this characteristic.

The comparisons for the three components of center of gravity acceleration are shown on figure 7. The normal and longitudinal accelerations show exceptional agreement. The shape and maximum values for both quantities are very well simulated by the analysis. During the test, some transverse acceleration is experienced during the impact of legs 2 and 3, while the analysis does not predict this acceleration. In the test, the lander actually has a .0175 rad. ($1^{\circ}$) yaw which produces this transverse acceleration. However, in the analysis, no yaw is included in the initial conditions. The primary strut stroke lengths are predicted exceptionally well by the analysis.

## Drop Case 13

In Drop Case 13 the original primary strut configuration having a full deadband was used. The initial landing conditions included the lander oriented for 1-2 landing, leg 1 pitched down .0873 rad. ($5^{\circ}$), and 1.219 mps (4 fps) uphill horizontal velocity.

Figures 8 and 9 show the strut forces and strokes, and the center of gravity acceleration time histories. The strut forces are predicted by the analysis exceptionally well. During leg 1 impact, the primary strut experiences a relatively long period in the deadband region while the compressive forces in the secondary struts continued to increase. This condition results in very high pitching rotation since the line of action for the secondary struts is projected above the center of gravity. The analysis simulates this condition very well.

For the impact of legs 2 and 3, the timing is excellent. Only the secondary strut forces for leg 2 are in disagreement with the test results indicating that a small compressive force occurs. In the test, the high friction is produced by placing a sheet of sandpaper on the landing surface and a rubber patch on the footpads. In every case, the sandpaper proceeded to tear loose during footpad impact, thus causing an appreciable reduction in the friction coefficient. Also note that the primary strut of leg 1 has a small spike force after the secondary struts unload. This force can be attributed to inertial effects of the footpad after it leaves the landing surface.

The three components of the center of gravity acceleration are in good agreement. The peaks for both analysis and test occur at the same times and their magnitudes are approximately the same. Note that the direction of the transverse acceleration reverses for both. The primary strut stroke lengths are in good agreement. Test results show that leg 1 strut re-extends through the deadband and then goes back to its maximum stroke length due to the pad's inertia.

The analysis predicts that the lander will be unstable on .2269 rad. ($13^{\circ}$) slope for these initial conditions. However, Case 14 shows that the actual lander is stable on .2793 rad. ($16^{\circ}$) slope. Two possible explanations of why the analysis predicts an unstable landing whereas the test shows the lander to be stable are: (1) an inertial force is recorded for leg 1 primary strut after it leaves the landing surface, thereby reducing the high pitch rate the lander has when

leg 1 left the surface, and (2) the secondary strut forces in legs 2 and 3 for the test are smaller than those for the analysis, indicating that the friction coefficient for the test is smaller than the value used in the analysis.

Drop Case 15

The strut configuration for Drop 15 has the bonded honeycomb primary struts, thus eliminating the deadband region. The initial conditions are similar to Drop Case 13. The strut force time histories are presented in figure 10. Both the analysis and test results are stable. The analysis predicts that the landing is unstable on a landing surface slope of .3491 rad. ($20^{\circ}$). Therefore, this landing is marginal for the analysis. The impact sequence and timing agreement are again very good. The most interesting characteristic of this landing is the leg 1 primary strut force. After the compressive force has been relieved, the strut experiences a small tensile force from the re-extension of the crushable honeycomb. In both the analysis and test, the bond breaks before the strut can unload. This small tensile force counter-balances the compressive force on the secondary struts, reducing the overturning torque that is observed for the full deadband strut. The strut forces for legs 2 and 3 show good agreement until the secondary struts forces are relieved. At this time, the sandpaper tears causing the friction to reduce. During the analysis, the friction coefficient is held constant at 1.0, thus the compressive forces of the secondary struts remain until the pads leave the landing surface. As with the previous case, this tearing of the sandpaper is believed to be a contributing factor in explaining why the analysis

predicts unstable landings on lower slopes than indicated by experiment.

The center of gravity accelerations show excellent agreement in all three components (figure 11). For both the normal and longitudinal accelerations, the test accelerations build up to the analytical values during legs 2 and 3 impact and then suddenly drop. This is attributed to the sliding of pads 2 and 3. The stroke lengths of the primary struts show good agreement with the analysis. Again the time history of leg 1 stroke length shows that the strut has re-extended to its initial length.

## Drop Case 17

Drop Case 17, with a ratchet installed on the primary strut, has approximately the same initial conditions as Drop Cases 13 and 15. Utilizing the ratchet configuration, the analysis predicts the lander is stable on a .6283 rad. ($36^{\circ}$) slope and unstable on .6458 rad. ($37^{\circ}$) slope. The test case is stable on a .5236 rad. ($30^{\circ}$) slope. The strut forces are shown on figure 12 and the comparison between analysis and test data is favorable. The time history of leg 1 struts indicate how the ratchet performs. After the compressive force in the primary strut is relieved, the strut re-extends until the ratchet reaches its nearest slot. After the ratchet engages, the strut experiences tensile force. The impact sequence and timing comparisons are good. In the experiment, legs 2 and 3 do not impact together, indicating that the lander has a small yaw rotation. In the analysis, this rotation is not accounted for, resulting in legs 2 and 3 impacting together.

The force levels and durations of the levels are in very good agreement as are the accelerations (figure 13). The analysis predicts no transverse acceleration since no initial yaw rotation is included. The stroke lengths for the primary struts exhibit very good agreement.

## PERFORMANCE SENSITIVITY OF THE MODEL

### Pitch Attitude

Drop Cases 2, 3, and 4 show the effects of the initial vehicle pitch attitude on the model. The pitch attitudes are $0^{\circ}$, .1658 rad. ($+9.5^{\circ}$), and -.1571 rad. ($-9^{\circ}$), for Cases 2, 3, and 4, respectively (see figures 16 through 21).

During the initial impact of leg 1, the primary strut exhibits approximately the same time histories for the three cases; however, the secondary struts differ considerably. In Case 3, where leg 1 is pitched up .1658 rad. ($+9.5^{\circ}$), the secondary struts experience only small compressive forces initially, which later change to tensile forces. In Case 2, with zero pitch attitude, the strut forces experience a time history in the form of a parabola with the maximum force approaching the limiters maximum elastic force. In Case 4, the strut force time histories indicate that the limiters experience plastic deformation. This difference in the secondary strut force time histories is directly attributed to the lander's attitude. The distance from the lander's center of gravity to the vertical line of action of leg 1's footpad is dependent upon the attitude of the lander. Using the nominal attitude Case 2 as the baseline, rotating leg 1 up or

counter-clockwise increases this distance and rotating leg 1 down decreases this distance. The amount of kinetic energy that is absorbed by leg 1 is inversely proportional to the normal distance from the center of gravity and the gravity vector at leg 1 footpad. Therefore, Case 4 has the largest secondary strut forces since the lander is pitched down.

The time between impacts of leg 1 and legs 2 and 3 is dependent on the attitude of the lander. The impacts of legs 2 and 3 occur at .10, .195, and .30 seconds after leg 1 impact for Cases 3, 2, and 4, respectively. It appears that the time between impact of the trailing and leading legs is directly proportional to pitch attitude and is about $\pm$.573 sec/rad ($\pm$.10 sec/deg) of pitch for the values of $V_V$, $V_H$, and $\alpha$ in these tests.

An interesting phenomenon is observed in struts 2L and 3R for all three cases. Upon impact, these struts experience small compressive forces before going into tension. At impact, the friction force is less than the tangential component of the pad force, thus allowing the pads to slide along the surface. As the friction force increases, the sliding decreases until the pad becomes stationary. To resist the friction force, the trailing struts, 2R and 3L, develop compressive forces. To balance these compressive forces in the trailing struts, the leading struts develop tensile forces.

The time histories of the body components of the center of gravity acceleration show that the magnitude of the maximum acceleration

experienced during the landing is approximately the same for all three cases, indicating that maximum acceleration is independent of the lander's attitude. The magnitudes of the maximum primary strut stroke lengths are approximately the same for all three cases.

### Horizontal Velocity

To examine the effects that horizontal velocity has on the lander's behavior, Drop Cases 4 and 8 are discussed together (figures 20, 21, 24, and 25). Both cases have approximately the same initial landing conditions except for the direction of the horizontal velocity vector - Case 4 has a 1.219 mps (4 fps) downhill velocity and Case 8 1.219 mps (4 fps) uphill velocity.

For Case 4 the primary strut reaches its second force level and the secondary struts experience some plastic deformation. All three struts unload at approximately 0.04 seconds. For Case 8 the primary strut force reaches its third force level before it unloads at 0.45 seconds. Notice that between $t = .045$ and $t = .05$ seconds, the primary strut is in the deadband region as the secondary struts continue to load in compression. Since the line of action for the secondary struts forces passes above the center of gravity, a compression force on these struts produces an overturning moment on the lander.

Comparisons of Cases 4 and 8 show that more energy is absorbed during leg 1 impact in Case 8, indicating that the lander in Case 8 has less kinetic energy when leg 1 leaves the surface. This suggests that the lander is more stable for Case 8. However, since the line

of action of the secondary struts passes above the center of gravity, the greater compressive forces in Case 8 produce more destabilizing angular momentum than in Case 4. This explains why the primary struts of legs 2 and 3 reach the fourth force level in Case 8 for both analysis and test.

The magnitude for leg 1 maximum stroke length is greater for Case 8 than Case 4 which is consistent with the discussion of leg 1 primary strut force. The magnitudes for legs 2 and 3 maximum stroke lengths are approximately the same for both cases.

By comparing the results from Cases 4 and 8, it is apparent that the horizontal velocity plays a very important role in the behavior of the lander. The leading leg experiences considerably more loading for landings with uphill velocity than for landings with downhill velocity. The timing sequence between the impact of leg 1 and legs 2 and 3 is affected by the horizontal velocity. The impact times for legs 2 and 3 are 0.29 and 0.22 seconds for case 4 and case 8, respectively. This difference is attributed to the higher angular rates developed in Case 8. On the basis of these results, it might be surmised that this design would be more unstable in a landing where the horizontal velocity was directed into the slope.

## Roll Attitude

Case 9 is similar to Case 8 except that the lander is rolled 3.142 rad. ($180^{\circ}$) so that legs 2 and 3 impact the landing surface initially

(a 2-1 landing). During legs 2 and 3 impact, approximately 90% of the lander's initial kinetic energy is dissipated. Therefore, during leg 1 impact, the secondary struts experience very small forces. The largest differences between these cases is in the lower angular velocity produced in Case 9. Since the angular velocity is dependent on the moment produced by the strut forces, the greater moment arm of Case 8 is a predominant factor.

### Primary Strut Configuration Effects on Stability

To show the effects of the primary strut configuration, Drop Cases 13, 14, 15, 16, and 17 are examined together. The three strut configurations are (1) with full deadband, (Cases 13 and 14); (2) with bonded honeycomb, (cases 15 and 16); and (3) with ratchet (Case 17). The computed surface slopes where the lander will become unstable for these cases are .2269 rad. ($13^{\circ}$), .3491 rad. ($19^{\circ}$), and .6458 rad. ($37^{\circ}$) for the full deadband strut, the bonded honeycomb strut, and the ratchet strut cases, respectively. In the cases having the full deadband strut, the strut experiences a relatively long period in the deadband region while the compressive forces in the secondary struts continued to increase during leg 1 impact. This situation results in very high destabilizing pitching rotation since the line of action for the secondary struts is projected above the lander's center of gravity. When the honeycomb is bonded to the primary struts, a tensile force is experienced by the strut due to the re-extension

of the crushable honeycomb. This tensile force reached a level high enough to break the bond. This force reduces the overturning torque observed in the full deadband strut cases, thereby increasing the critical stability slope. However, with the addition of the ratchet on the primary strut, the strut experiences large elastic tensile forces which reduce the overturning torque so that this type of landing condition becomes very stable.

## CONCLUSIONS

In evaluating the landing stability of the VL, two significant factors have been identified. One is that elimination of the strut deadband increases the stability of the lander. The other is that stability is very dependent on the direction of the horizontal velocity with respect to the surface slope. Landings having the horizontal velocity toward the landing surface are unstable at lower landing slope angles than those having the horizontal velocity directed away from the surface.

No attempt was made to fully simulate the test drop results. Certain assumptions in the analysis precluded exact correlation. Some of the more important assumptions involved the structural dynamics of lander center body, constant coefficient of friction for the footpads, and load transmission from the surface to the lander body. In general, however, the simulation program is shown to be capable of satisfactorily predicting loads and accelerations but is somewhat conservative in lander stability predictions.

## REFERENCES

1. Muraca, Ralph J.; Campbell, Janet W.; and King, C. Anderson: A Monte Carlo Analysis of the Viking Lander Dynamics. NASA TN D-7959.

2. McGehee, John R.; and Stubbs, Sandy M.: Experimental Validation of a Landing-Dynamics Computer Program for Legged Spacecraft Landers. NASA TN D-7301, December 1973.

TABLE 1

3/8 SCALE VIKING DROP TEST

INITIAL CONDITIONS FOR DROPS

| DROP NO. | VERT. VEL ($V_V$) mps (fps) | HORIZ. VEL ($V_H$) mps (fps) | ROLL ($\psi$) RAD. (Deg) | PITCH ($\theta$) RAD. (Deg) | YAW ($\phi$) RAD. (Deg) | SLOPE ($\alpha$) RAD. (Deg) | FRICT. COEF. $\mu$ | STRUT* TYPE |
|---|---|---|---|---|---|---|---|---|
| 1 | 4.017 (13.18) | 0 | 0 | -0.0087 (-1/2) | 0 | 0 | 0.577 | 1 |
| 2 | 3.420 (11.22) | -1.219 (-4.0) | 0 | 0 | 0 | 0.3491 (20) | 0.577 | 1 |
| 3 | 3.438 (11.28) | -1.219 (-4.0) | 0 | 0.1658 (9-1/2) | -0.0087 (-1/2) | 0.3491 (20) | 0.577 | 1 |
| 4 | 3.106 (10.19) | -1.219 (-4.0) | 0 | -0.1571 (-9) | 0.0175 (1) | 0.3491 (20) | 0.577 | 1 |
| 5 | 3.548 (11.64) | -1.219 (-4.0) | 2.618 (150) | 0 | 0 | 0.3491 (20) | 0.577 | 1 |
| 6 | 3.066 (10.06) | -1.219 (-4.0) | 0 | -0.1484 (-8-1/2) | 0 | 0.3491 (20) | $\infty$ | 1 |
| 7 | 3.362 (11.03) | -1.219 (-4.0) | 0 | 0.1745 (10) | -0.0175 (-1) | 0.3491 (20) | $\infty$ | 1 |
| 8 | 3.322 (10.90) | 1.219 (4.0) | 0 | -0.1571 (-9) | 0.0087 (+1/2) | 0.3491 (20) | 0.577 | 1 |
| 9 | 3.655 (11.99) | 1.219 (4.0) | 3.142 (180) | 0.1571 (9) | 0 | 0.3491 (20) | 0.577 | 1 |
| 10 | 3.353 (11.0) | 0 | 0 | 0.0087 (+1/2) | -0.0175 (-1) | 0.5760 (33) | 0.577 | 1 |
| 11 | 3.322 (10.9) | 0 | 0 | 0.0044 (+1/4) | -0.0262 (-1-1/2) | 0.5760 (33) | 1.0 | 1 |
| 12 | 3.353 (11.0) | 0 | 0 | 0.0044 (+1/4) | -0.0218 (-1-1/4) | 0.6109 (35) | 0.577 | 1 |
| 13 | 3.353 (11.0) | 1.219 (4.0) | 0 | -0.0960 (-5-1/2) | 0.0131 (+3/4) | 0.3316 (19) | 1.0 | 1 |
| 14 | 3.353 (11.0) | 1.219 (4.0) | 0 | -0.0829 (-4-3/4) | 0 | 0.2793 (16) | 1.0 | 1 |
| 15 | 3.292 (10.8) | 1.219 (4.0) | 0 | -0.0916 (-5-1/4) | -0.0044 (-1/4) | 0.3316 (19) | 1.0 | 2 |
| 16 | 3.353 (11.0) | 1.219 (4.0) | 0 | -0.0916 (-5-1/4) | 0 | 0.5236 (30) | 1.0 | 2 |
| 17 | 3.353 (11.0) | 1.219 (4.0) | 0 | -0.0960 (-5-1/2) | 0 | 0.5236 (30) | 1.0 | 3 |
| 18** | 3.353 (11.0) | 1.219 (4.0) | 2.094 (120) | 0.0401 (2.3) | -0.0777 (-4.45) | 0.3142 (18) | 1.0 | 1 |

*STRUT TYPE -

(1) WITH FULL DEADBAND
(2) WITH BONDED HONEYCOMB - NO DEADBAND
(3) WITH RATCHET - 0.00254 m (0.1 inches) DEADBAND

**C.G. OFFSET - 0.01524 m (0.6") TOWARD LEG $1_2$

$I_{xx}$ = 1.608 kg-$m^2$ (1.186 slug-$ft^2$)

$I_{yy}$ = 1.3312 kg-$m^2$ (0.98326 slug-$ft^2$)

$I_{zz}$ = 2.24724 kg-$m^2$ (1.65748 slug-$ft^2$)

TABLE 2

STABILITY DATA FOR 3/8 SCALE STABILITY DROP CASES

| DROP | VERTICAL VELOCITY ($V_V$) mps (fps) | VELOCITY ($V_H$) mps (fps) | TYPE OF LANDING | PITCH ($\theta$) RAD. (Deg) | FRICTION COEF. $\mu$ | SURFACE SLOPE ($\alpha$) RAD. (Deg) | TYPE OF STRUT | TEST S/U | STABILITY ANAL. PREDICTION S/U RAD. (Deg) |
|---|---|---|---|---|---|---|---|---|---|
| 10 | 3.353 (11.0) | 0 (0) | 1-2 | .0087 (+1/2) | .577 | .5760 (33) | 1 | S | .5934/.6109 (34/35) |
| 11 | 3.322 (10.9) | 0 (0) | 1-2 | .0044 (+1/4) | 1.0 | .5760 (33) | 1 | U | .5061/.5236 (29/30) |
| 12 | 3.353 (11.0) | 0 (0) | 1-2 | .0044 (+1/4) | .577 | .6109 (35) | 1 | U | .5934/.6109 (34/35) |
| 13 | 3.353 (11.0) | 1.219 (4.0) | 1-2 | -.0960 (-5-1/2) | 1.0 | .3316 (19) | 1 | U | .2094/.2269 (12/13) |
| 14 | 3.353 (11.0) | 1.219 (4.0) | 1-2 | -.0829 (-4-3/4) | 1.0 | .2793 (16) | 1 | S | .2094/.2269 (12/13) |
| 15 | 3.292 (10.8) | 1.219 (4.0) | 1-2 | -.0916 (-5-1/4) | 1.0 | .3316 (19) | 2 | S | .3316/.3491 (19/20) |
| 16 | 3.353 (11.0) | 1.219 (4.0) | 1-2 | -.0916 (-5-1/4) | 1.0 | .5236 (30) | 2 | U | .3316/.3491 (19/20) |
| 17 | 3.353 (11.0) | 1.219 (4.0) | 1-2 | -.0960 (-5-1/2) | 1.0 | .5236 (30) | 3 | S | .6283/.6458 (36/37) |
| 18 | 3.353 (11.0) | 1.219 (4.0) | 1-2 | -.0872 (-5) | 1.0 | .3142 (18) | 1 | U | . |

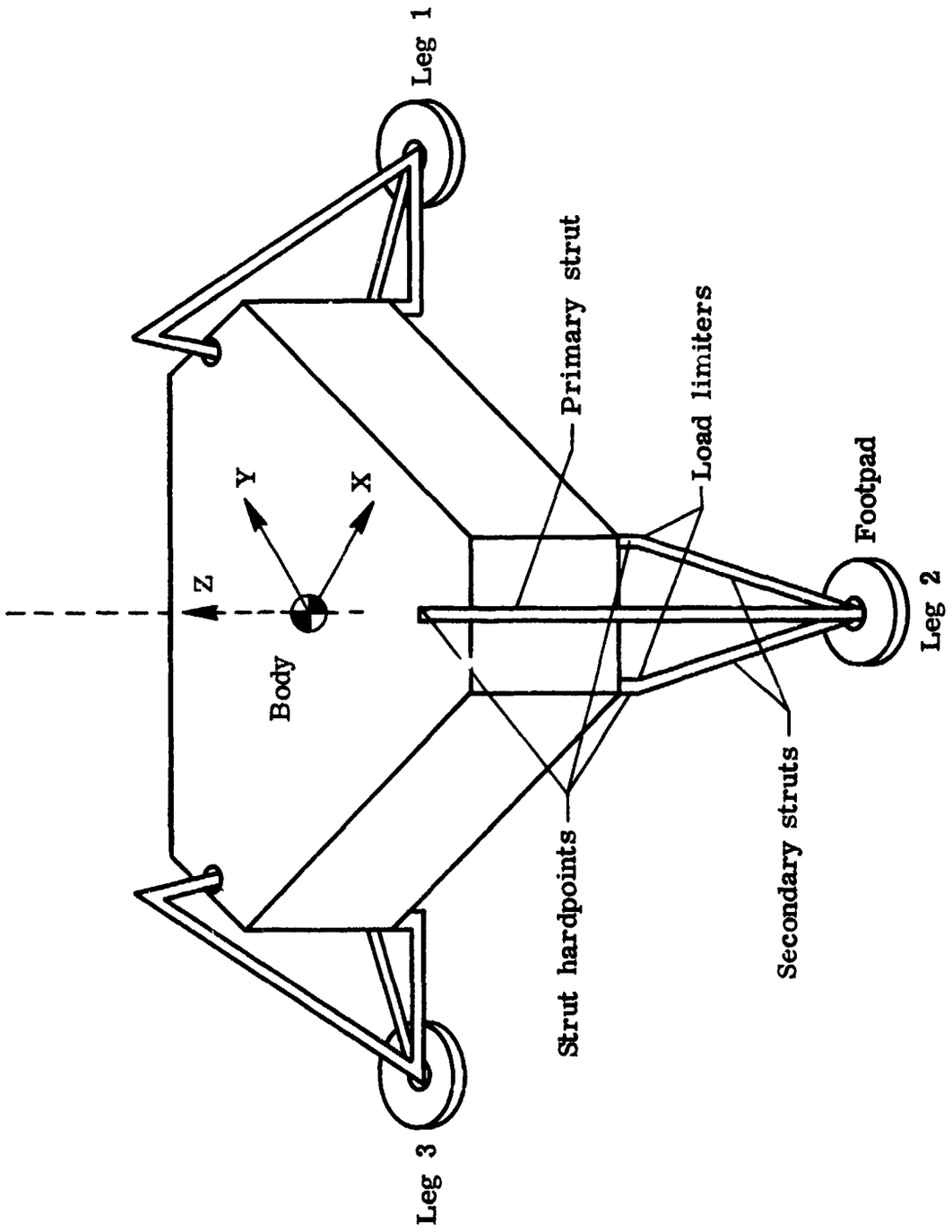


Figure 1.- Schematic of the Viking Lander Center Body, Legs, and Footpads.

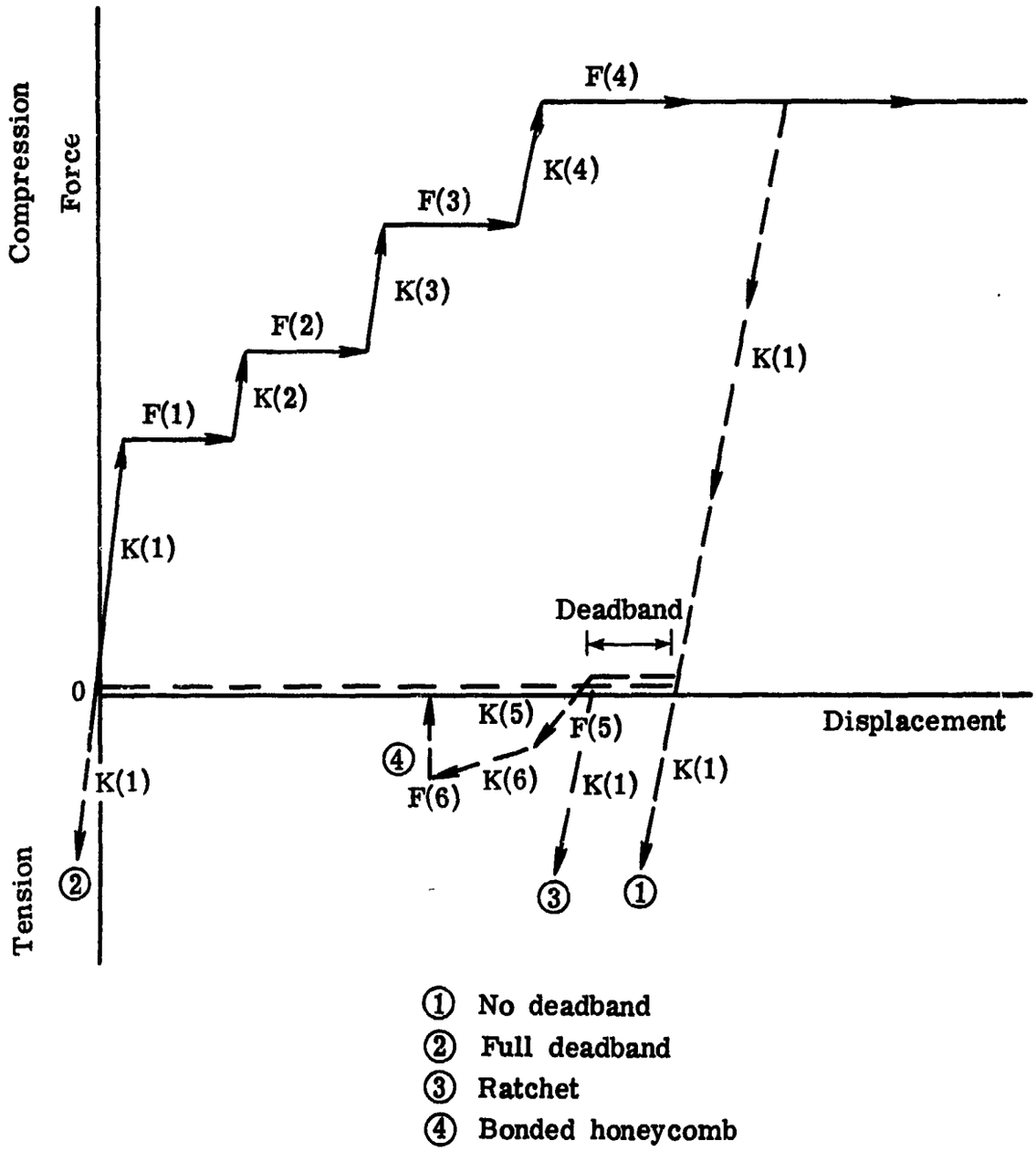


Figure 2.- Primary Strut Load/Stroke Characteristics.

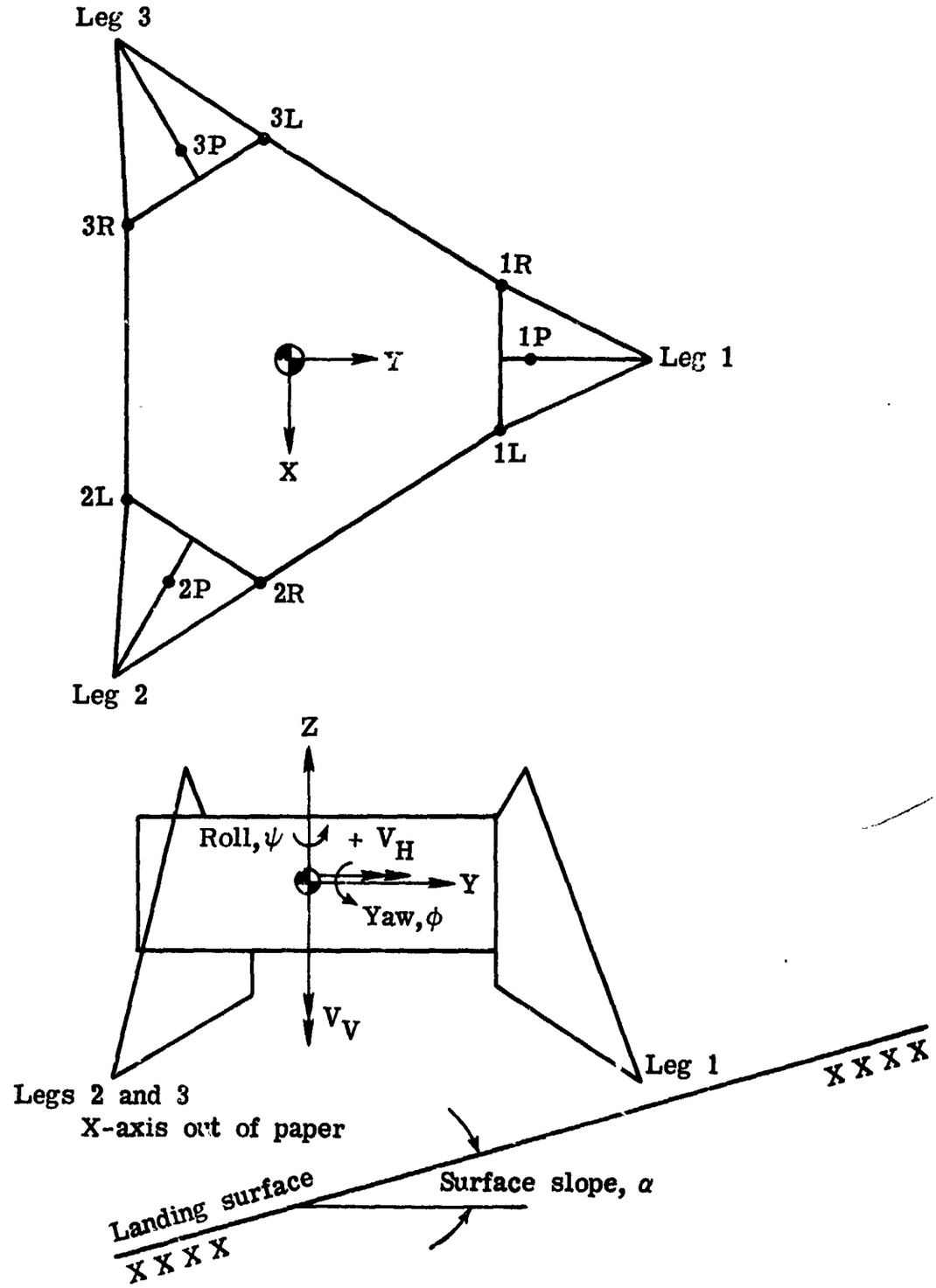


Figure 3.- Definition of Sign Convention of Initial Landing Conditions for 3/8 Verification.

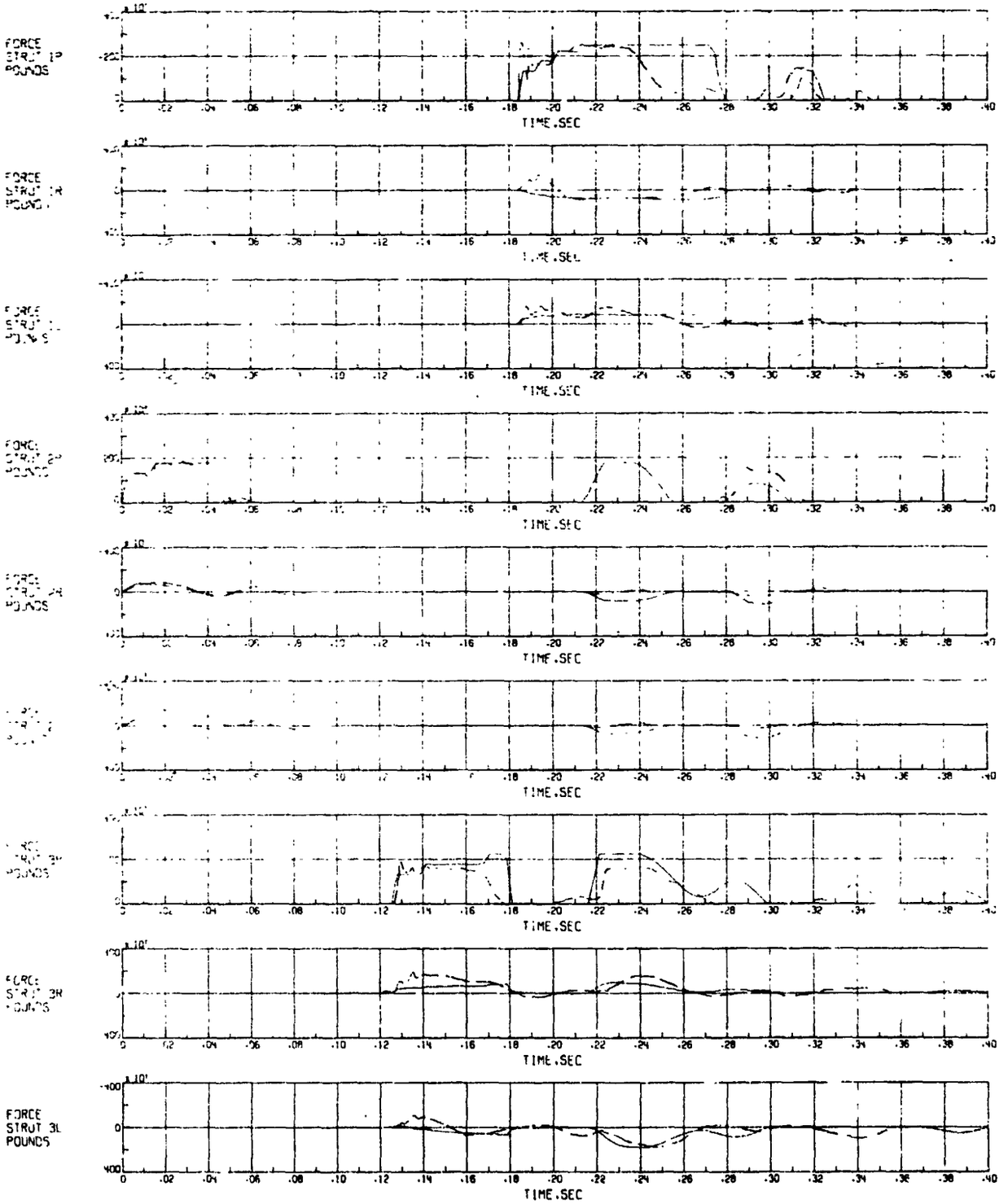


Figure 4.- Strut Forces versus Time - Drop Case 5.

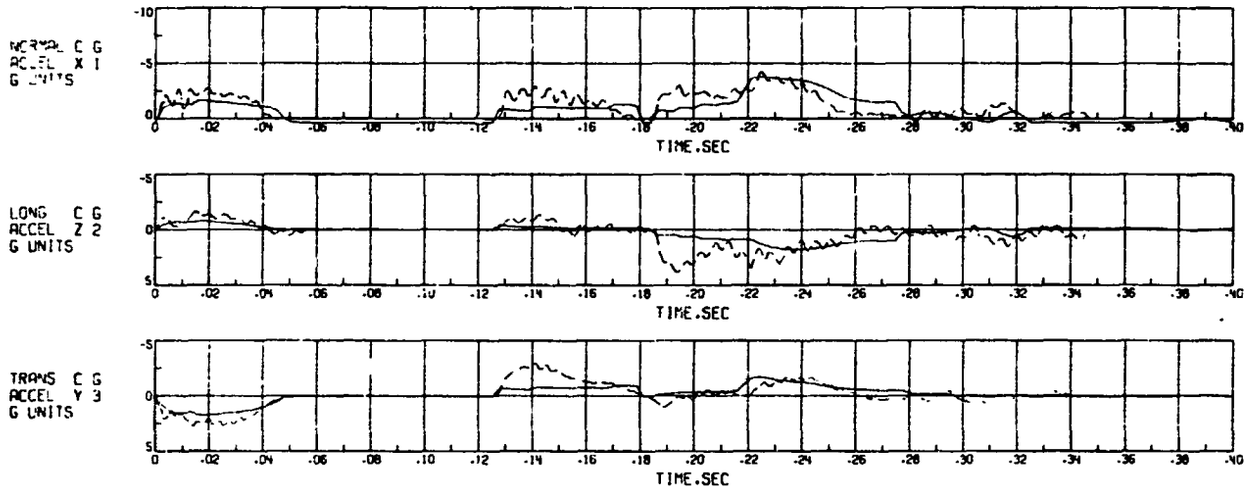


ORIGINAL PAGE IS
OF POOR QUALITY

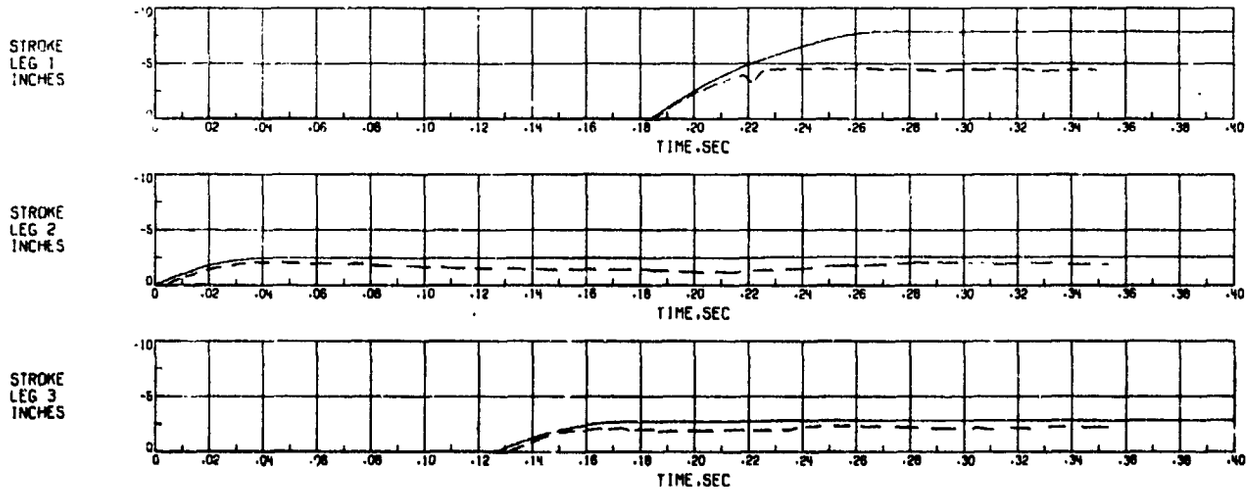


Figure 5.- Accelera⁺ions and Strokes versus Time - Drop Case 5.


Figure 6.- Strut Forces versus Time - Drop Case 7.

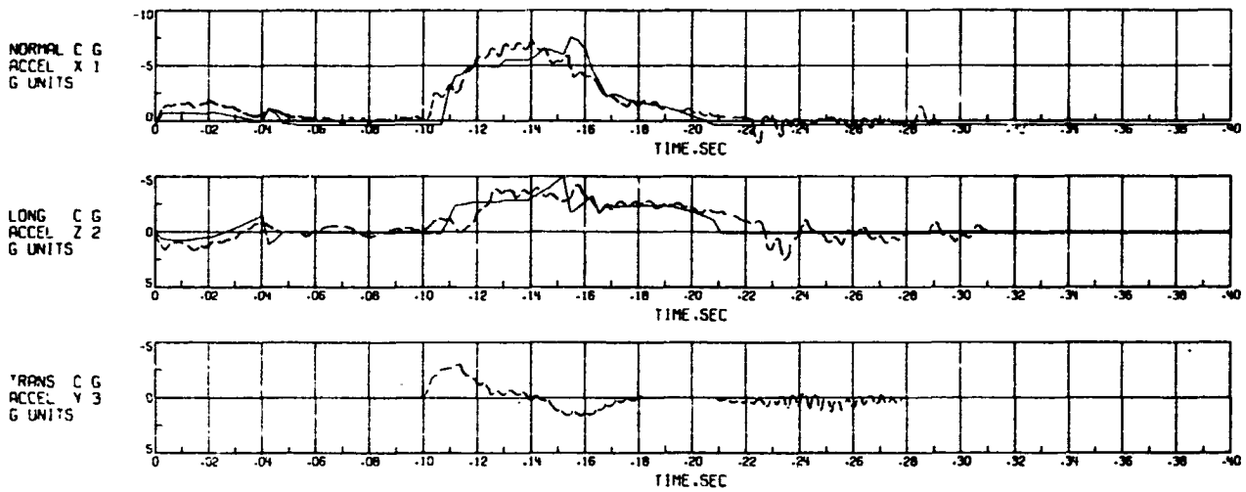




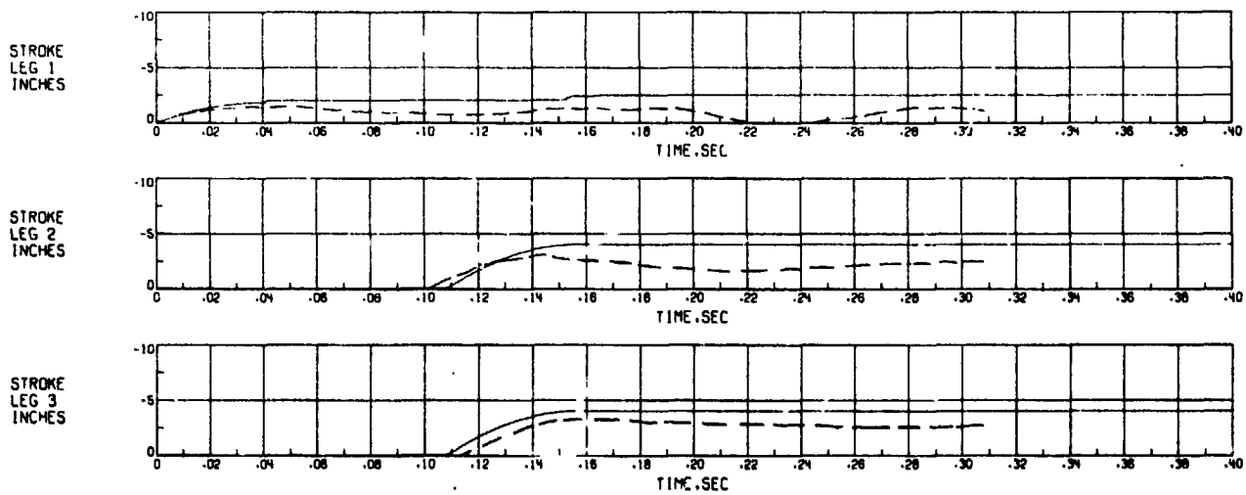


Figure 7.- Accelerations and Strokes versus Time - Drop Case 7.


Figure 8.- Strut Forces versus Time - Drop Case 13.

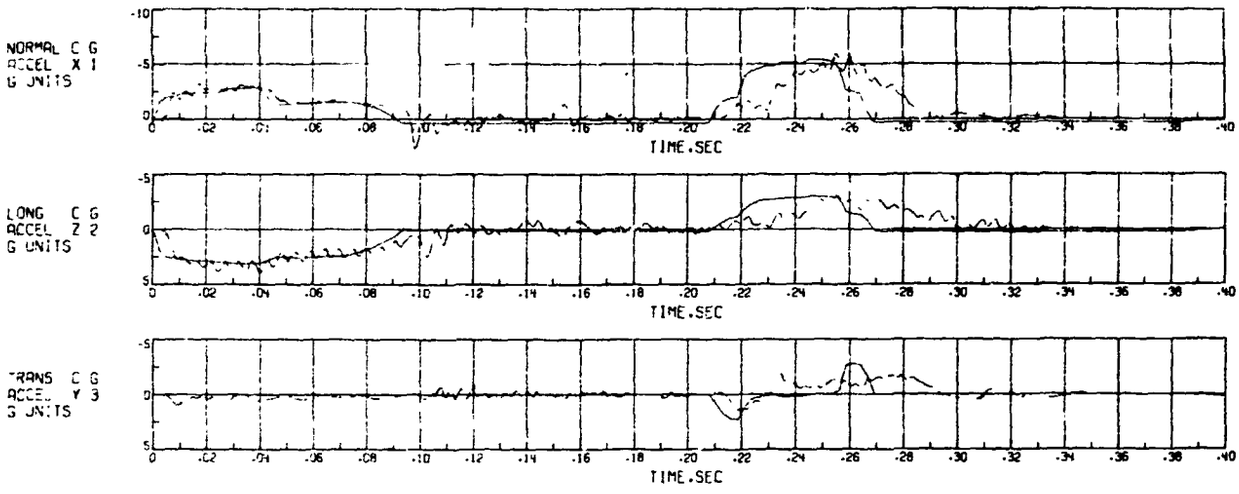




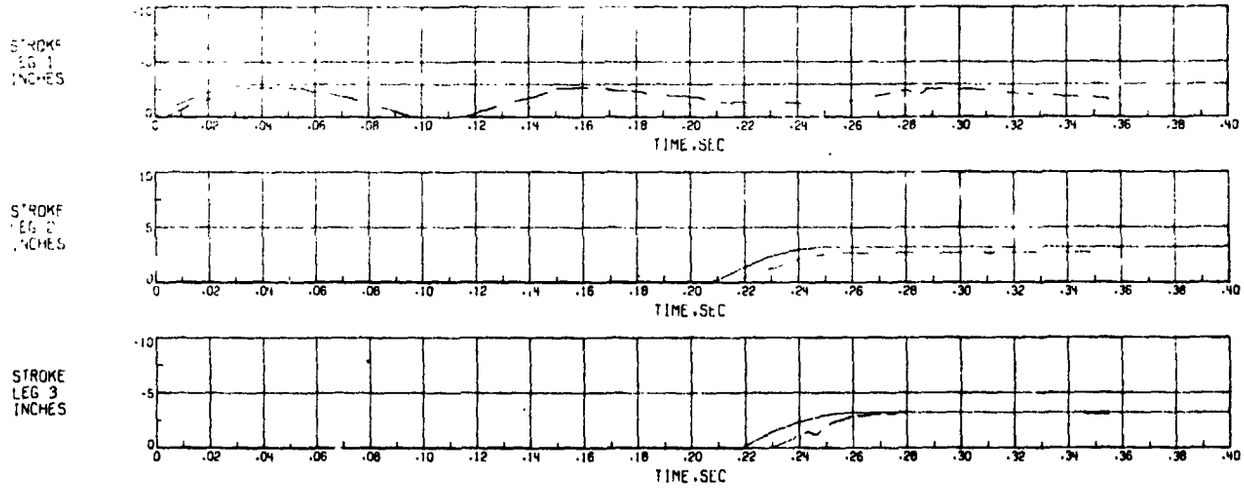


Figure 9.- Accelerations and Strokes versus Time - Drop Case 13.

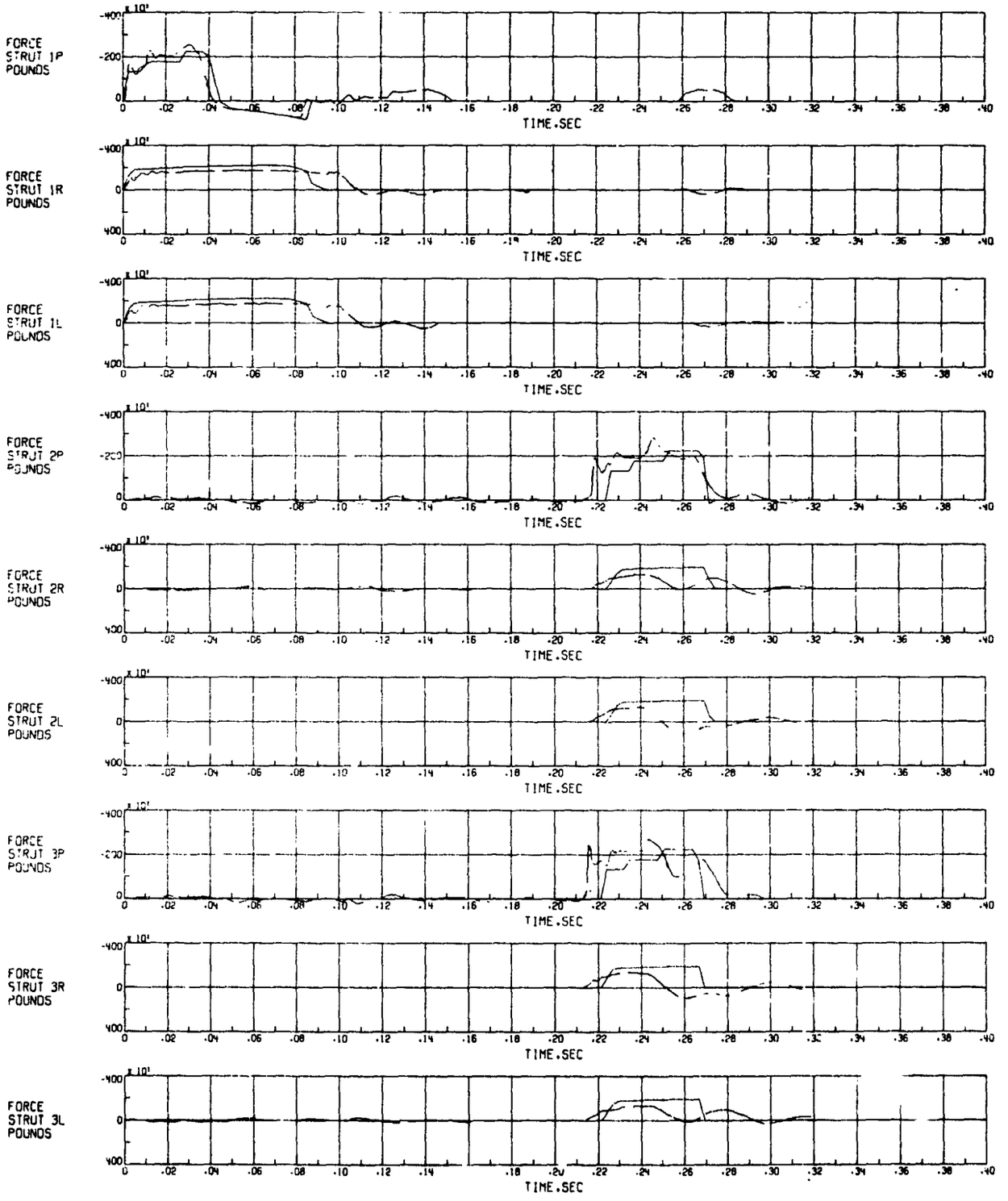


Figure 10.- Strut Forces versus Time - Drop Case 15.

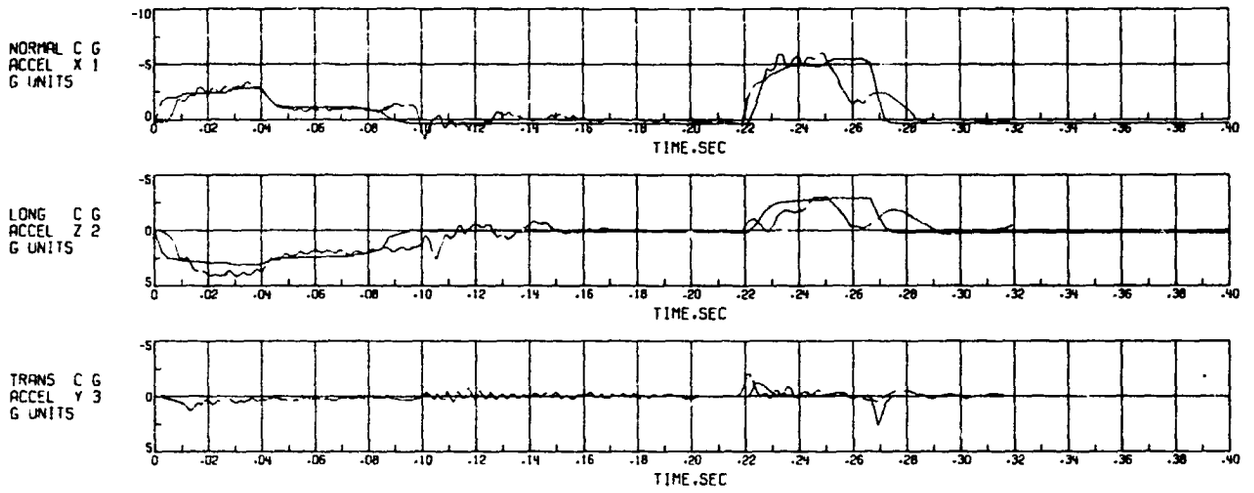




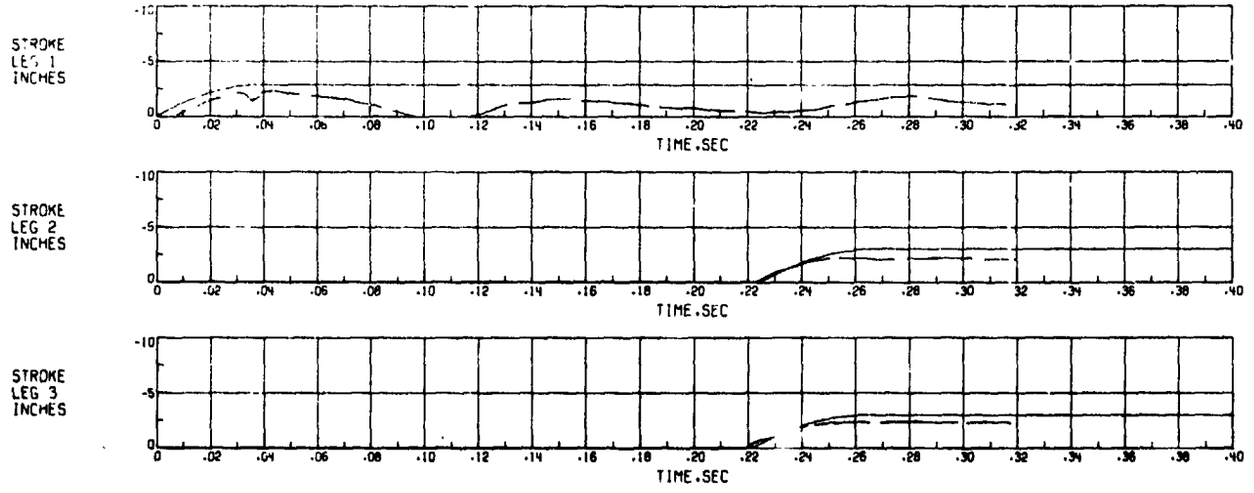


Figure 11.- Acceleration and Strokes versus Time - Drop Case 15.

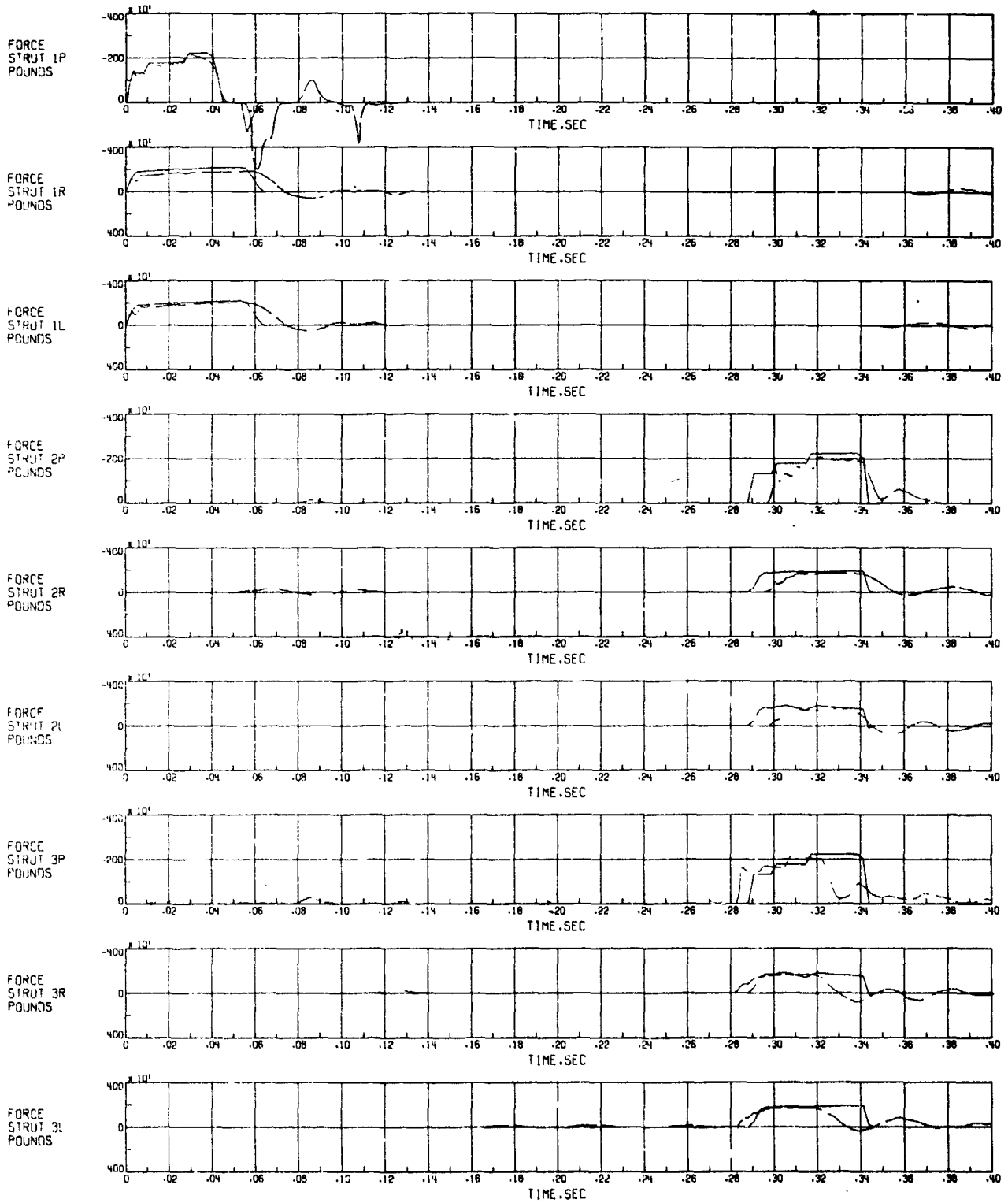


Figure 12.- Strut Forces versus Time - Drop Case 17.

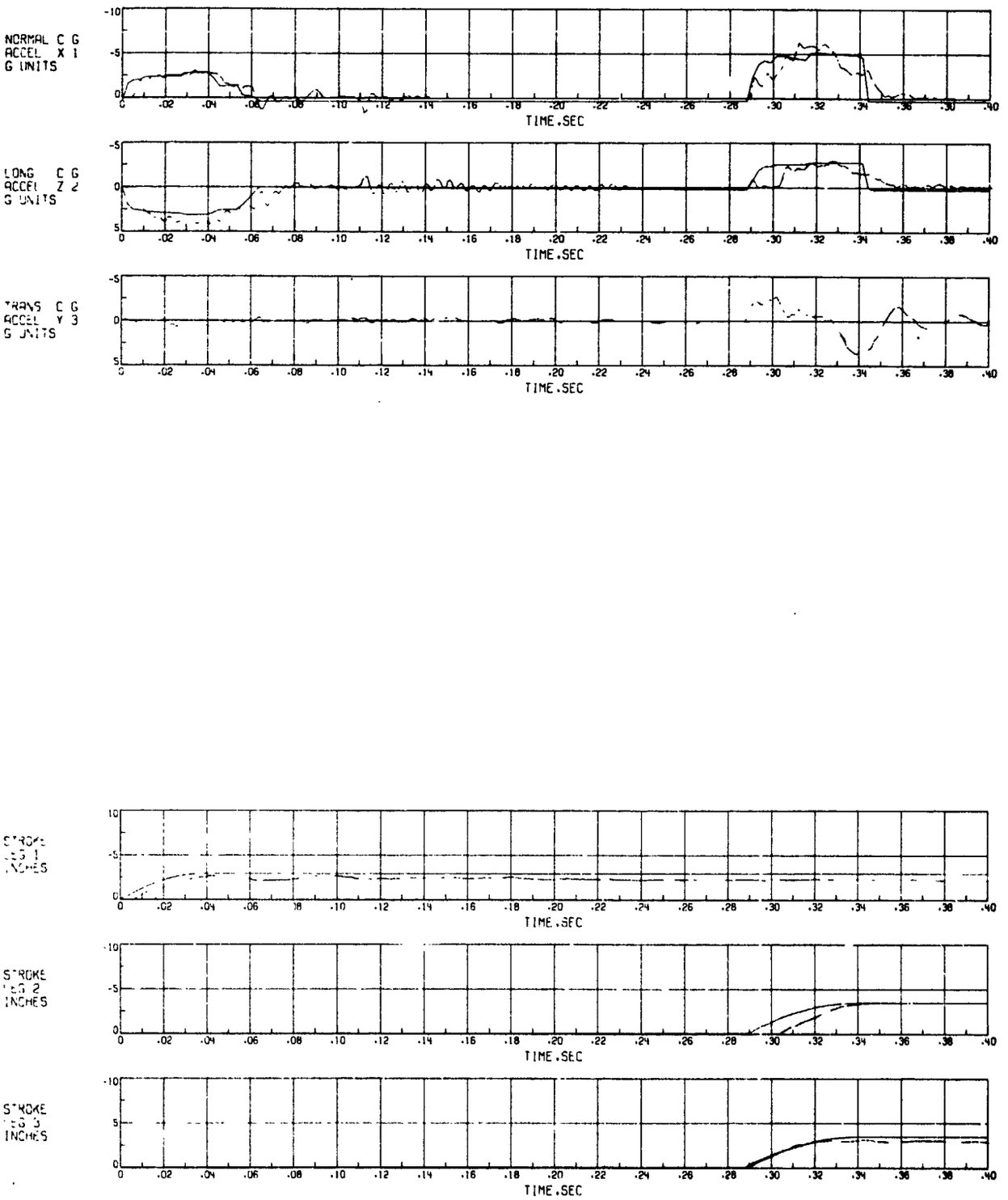


Figure 13.- Accelerations and Strokes versus Time - Drop Case 17.

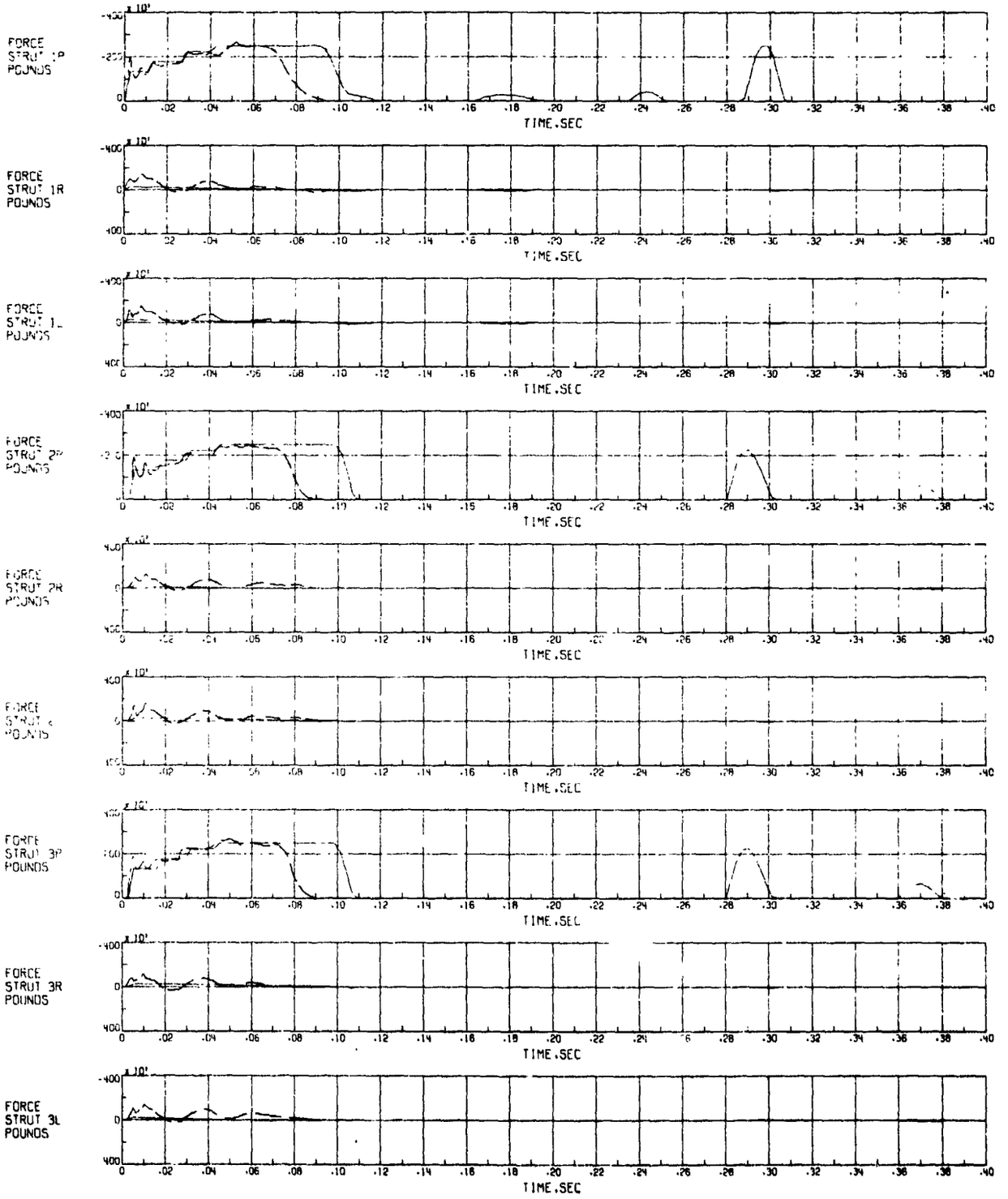


Figure 14.- Strut Forces versus Time - Drop Case 1.

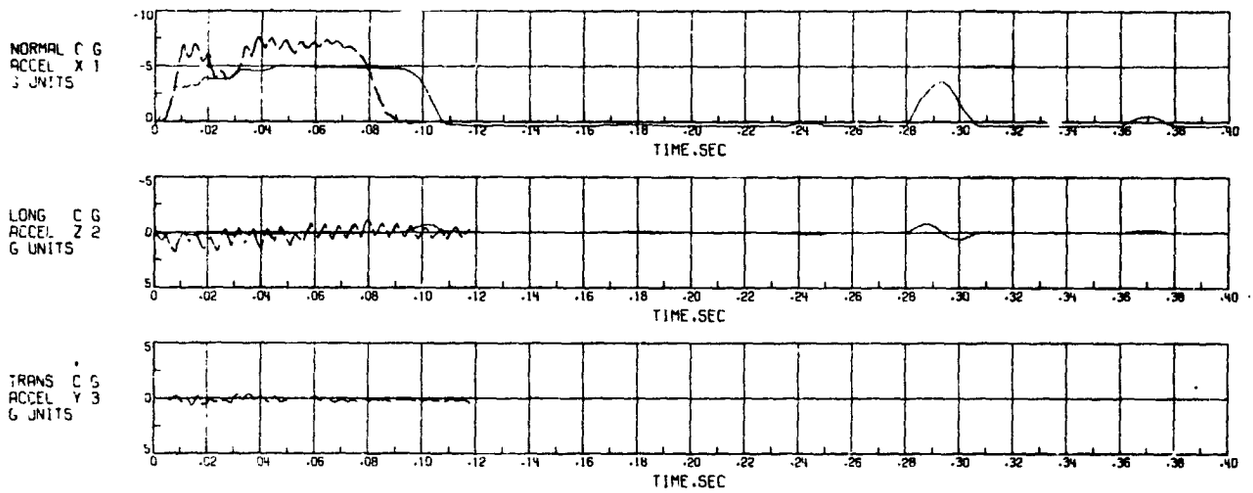




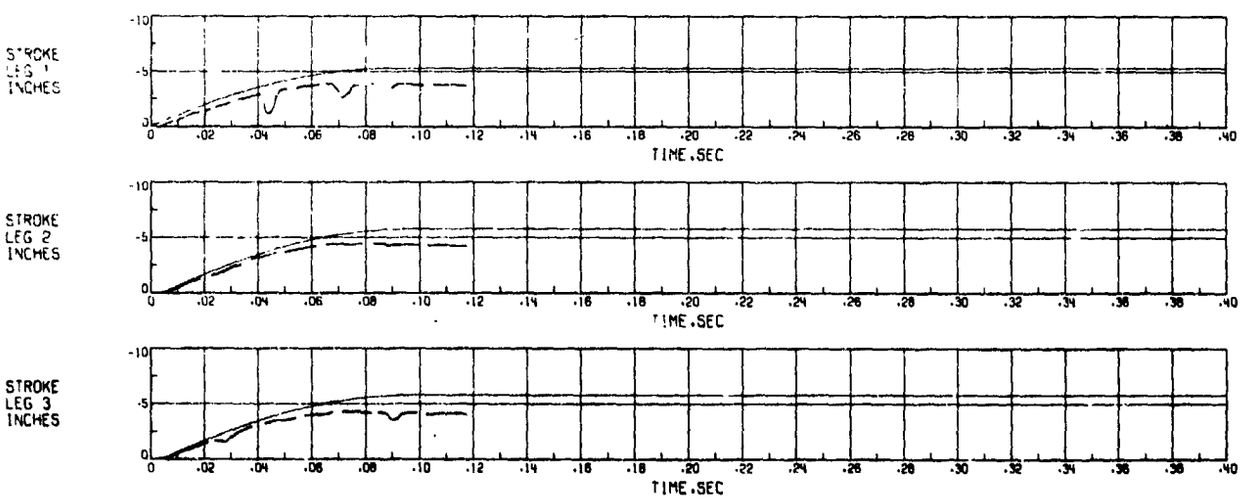


Figure 15.- Accelerations and Strokes versus Time - Drop Case 1.

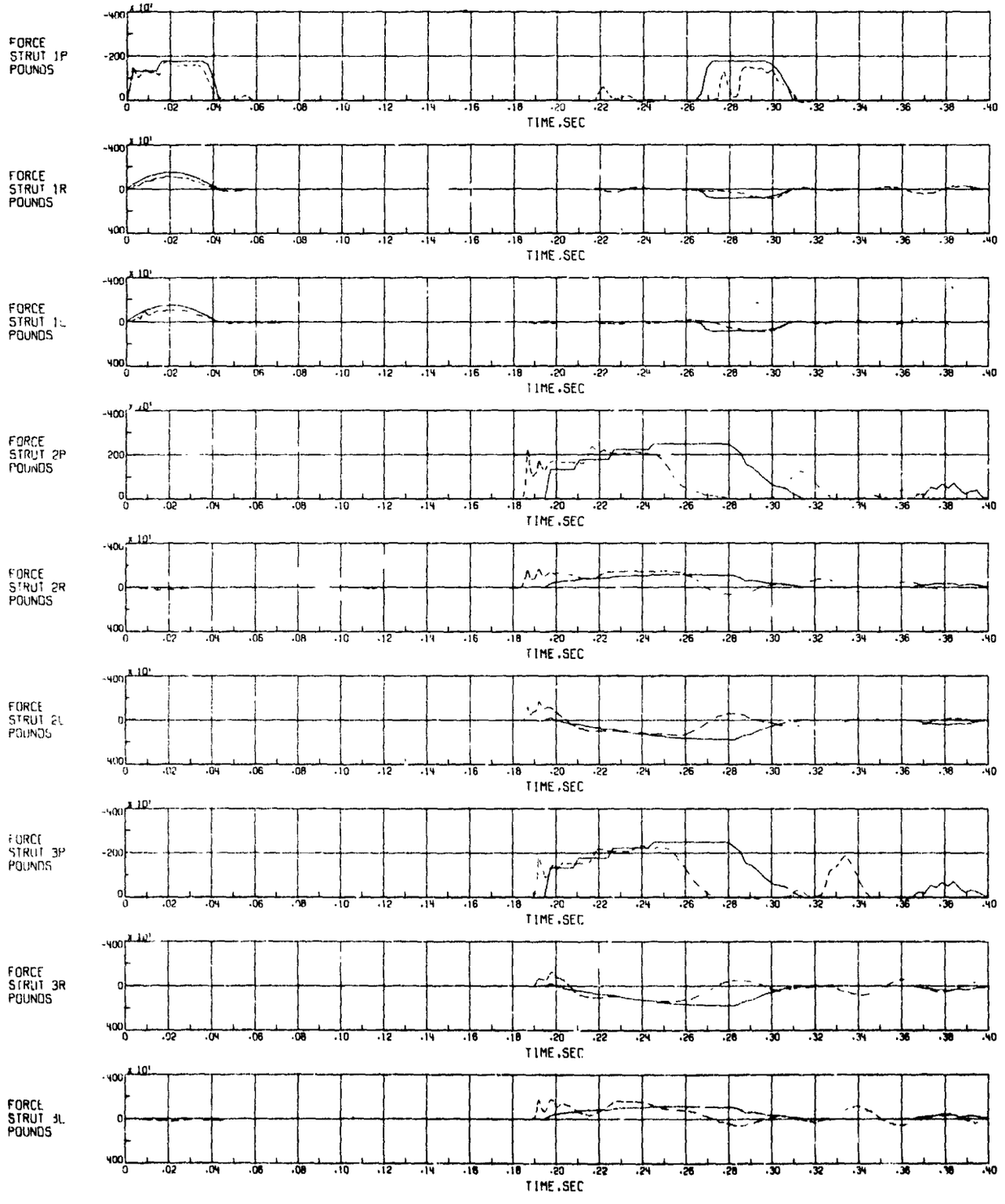


Figure 16.- Strut Forces versus Time - Drop Case 2.

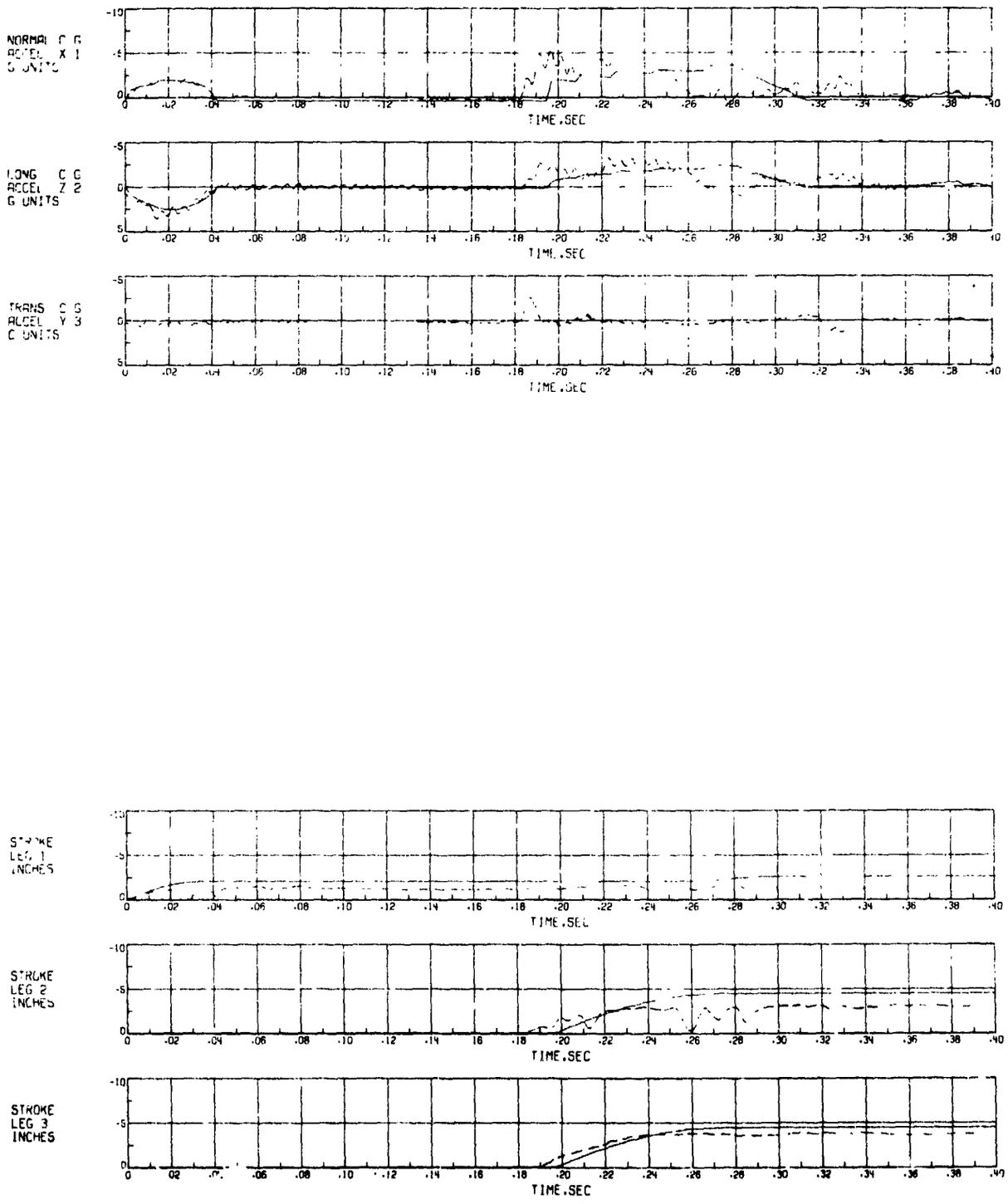


Figure 17.- Accelerations and Strokes versus Time - Drop Case 2.


Figure 18.- Strut Forces versus Time - Drop Case 3.

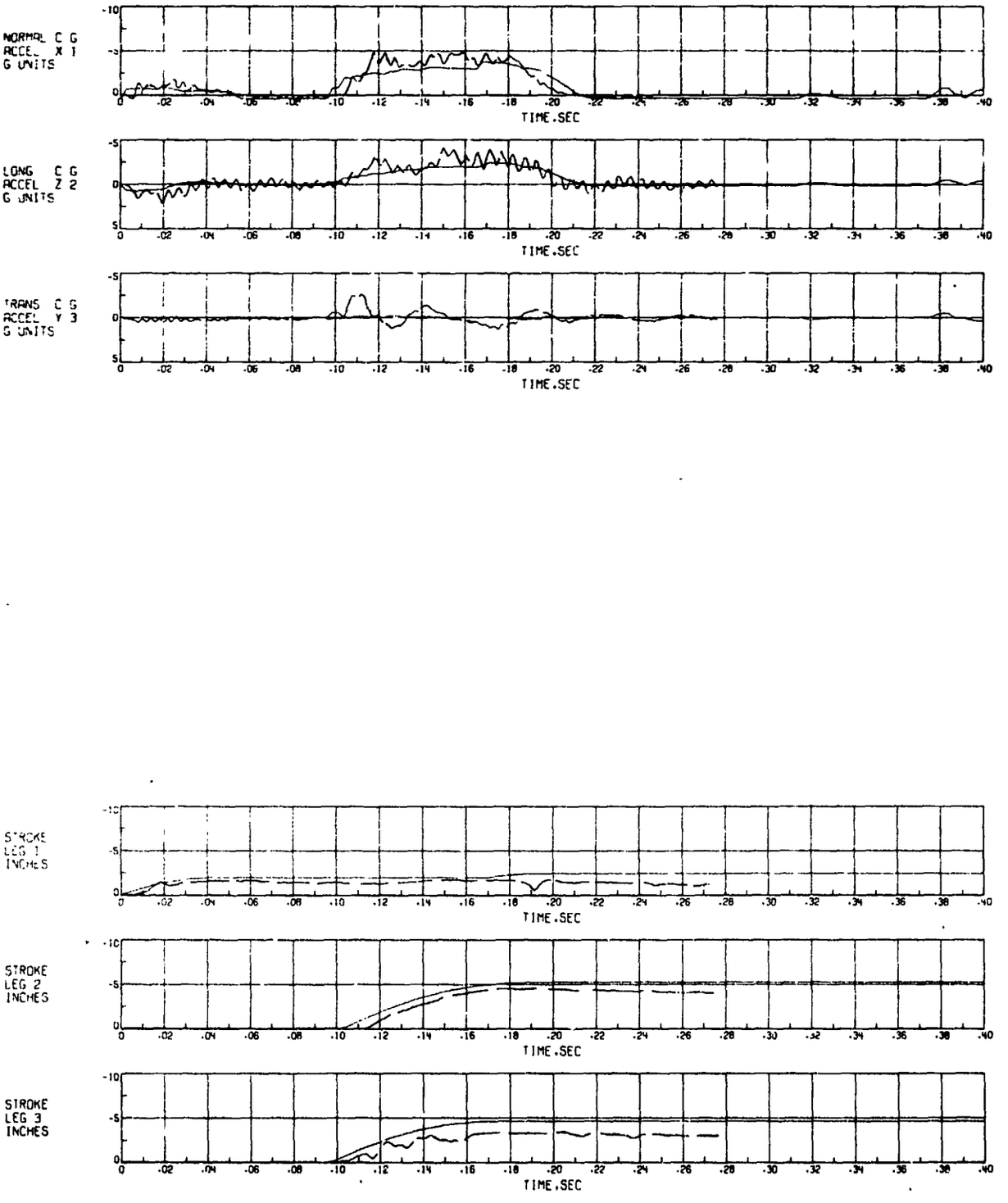


Figure 19.- Accelerations and Strokes versus Time - Drop Case 3.

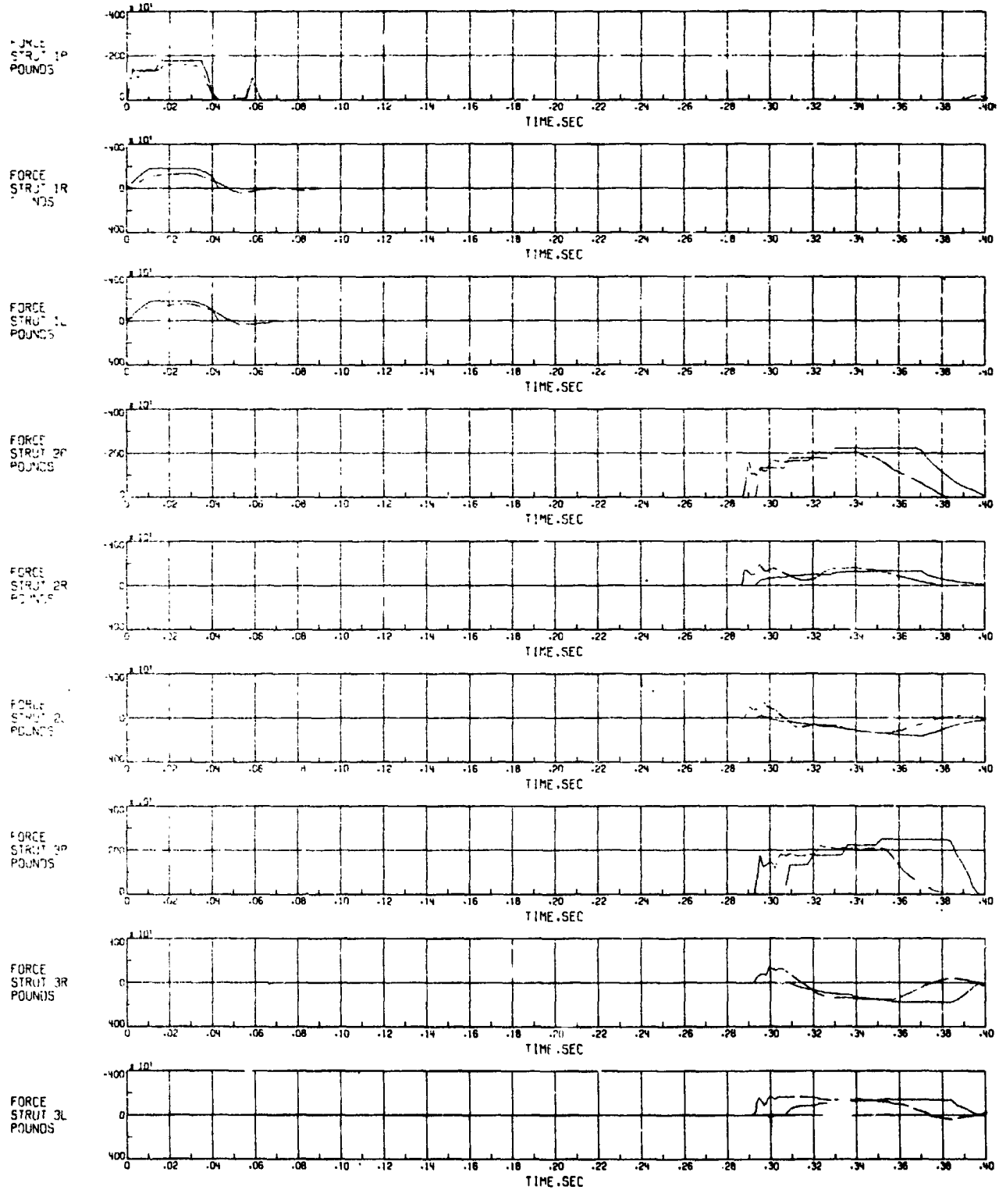


Figure 20.- Strut Forces versus Time - Drop Case 4.

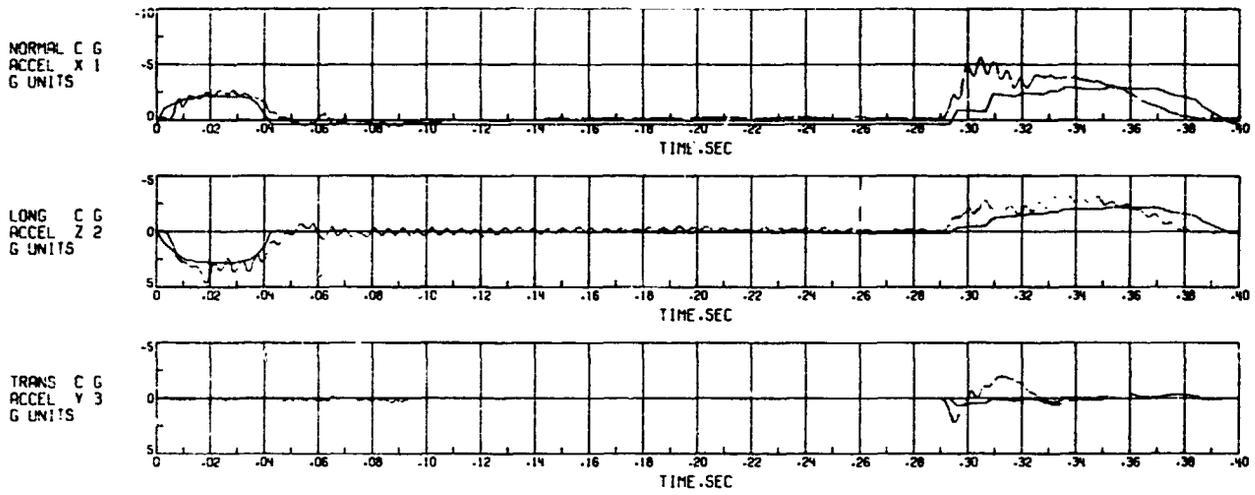




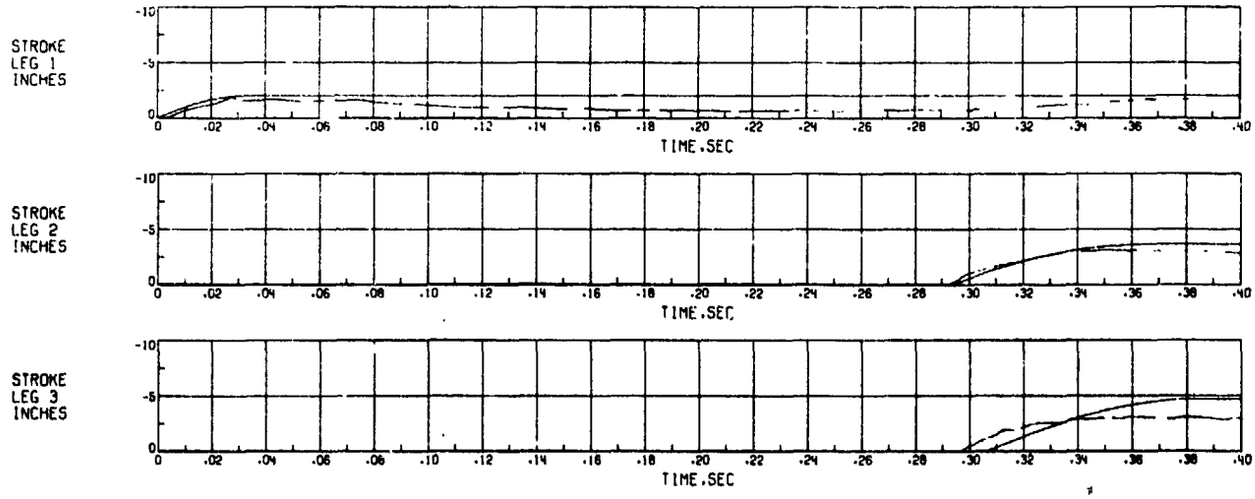


Figure 21.- Accelerations and Strokes versus Time - Drop Case 4.

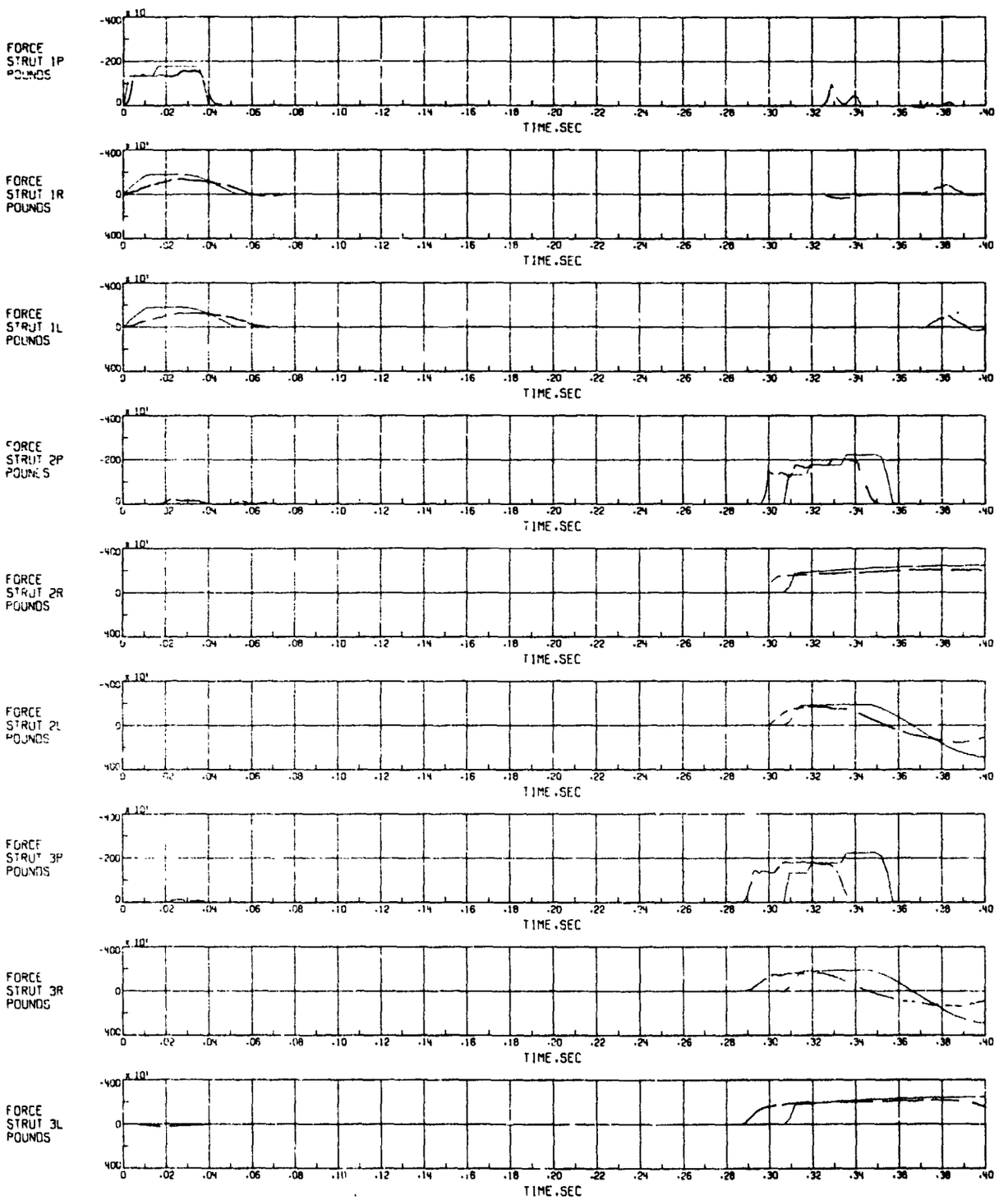


Figure 22.- Strut Forces versus Time - Drop Case 6.

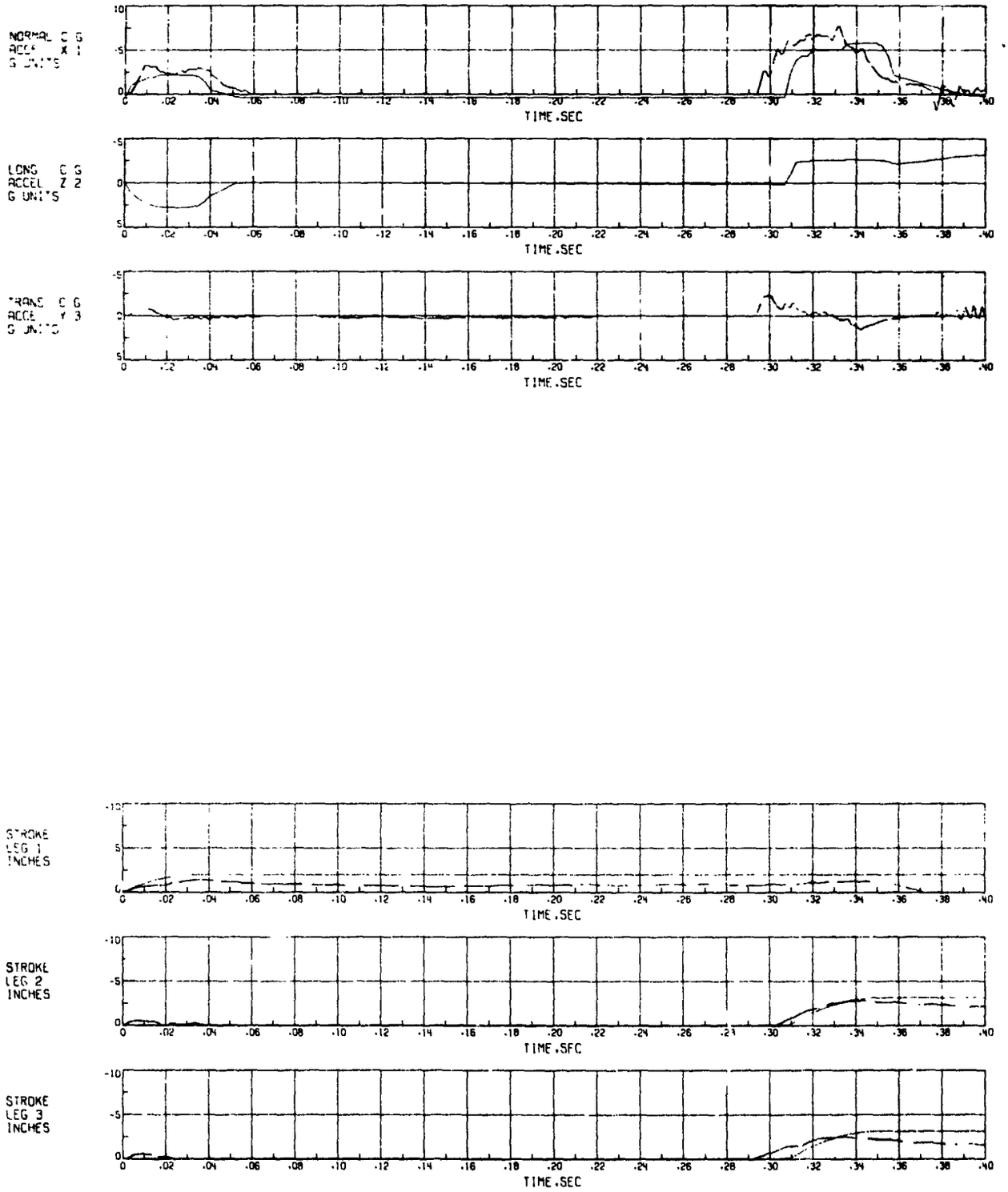


Figure 23.- Accelerations and Strokes versus Time - Drop Case 6.

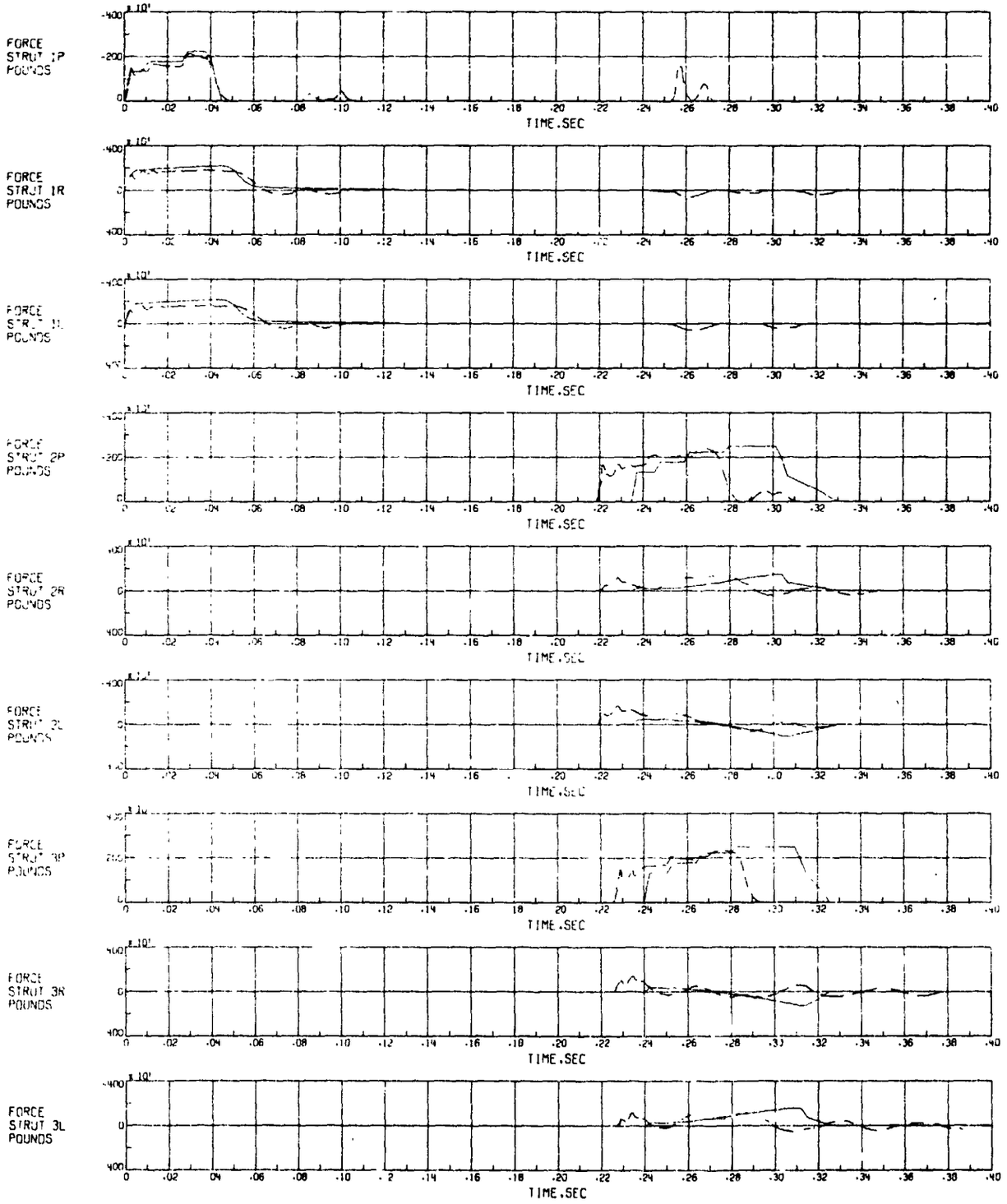


Figure 24.- Strut Forces versus Time - Drop Case 8.

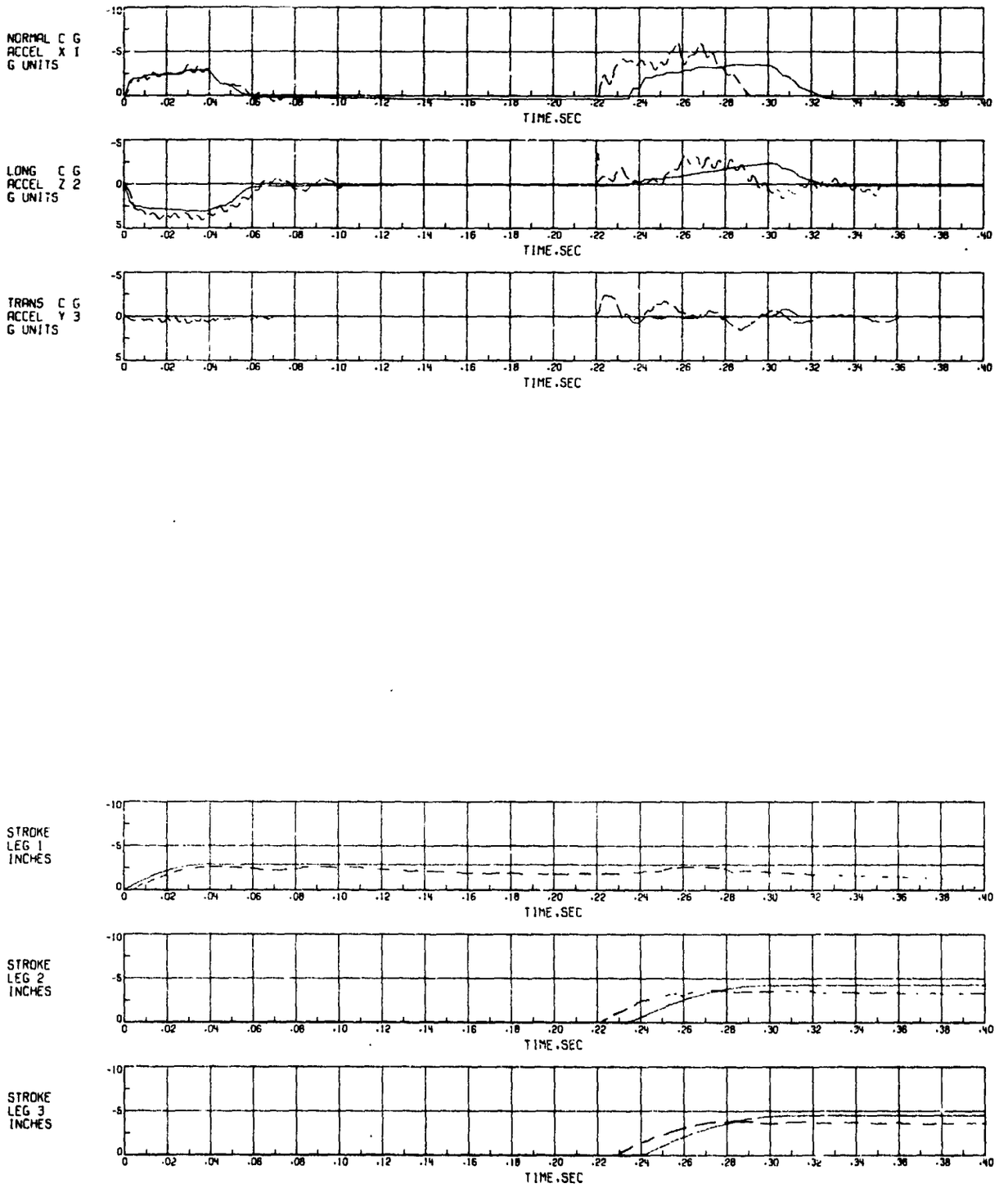


Figure 25.- Accelerations and Strokes versus Time - Drop Case 8.


Figure 26.- Strut Forces versus Time - Drop Case 9.

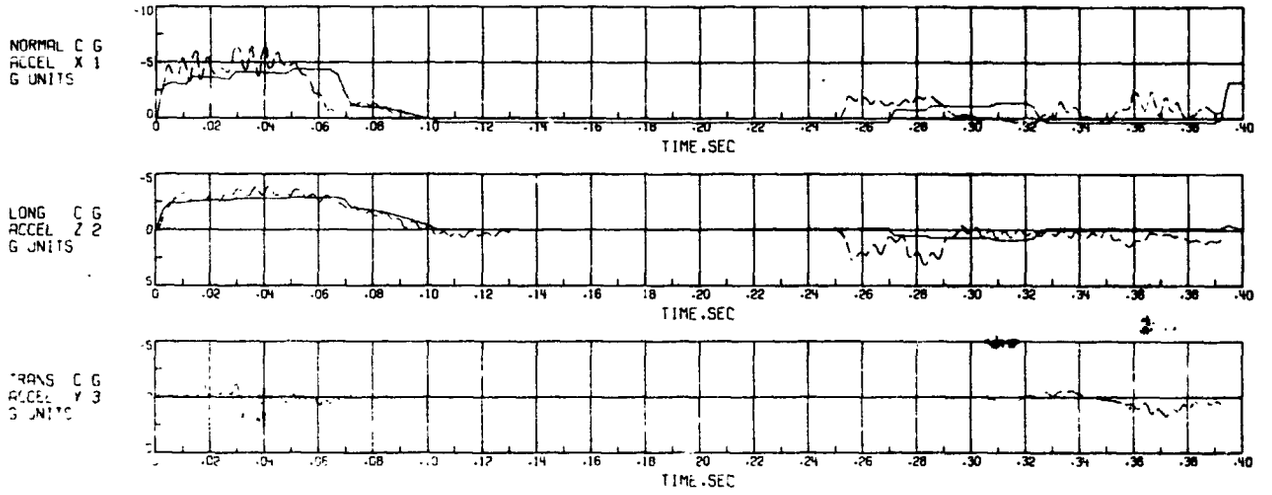


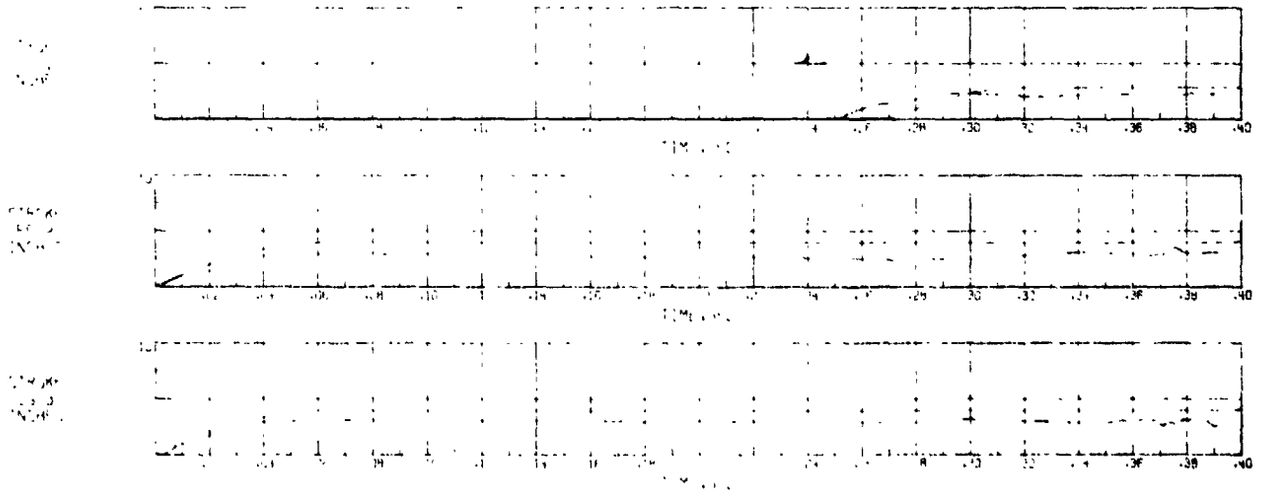

Figure 27.- Accelerations and Strokes versus Time - Drop Case 9.

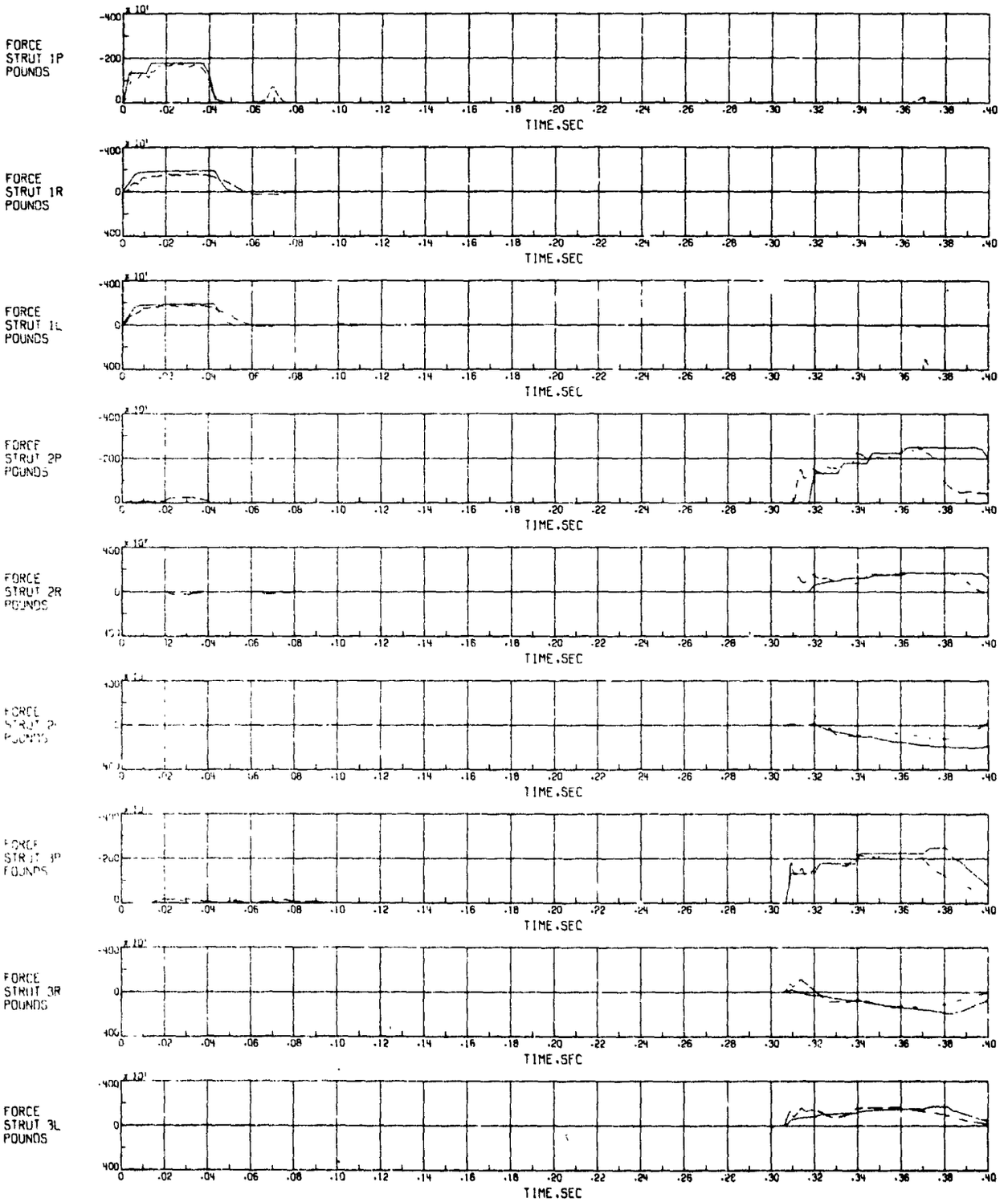


Figure 28.- Strut Forces versus Time - Drop Case 10.

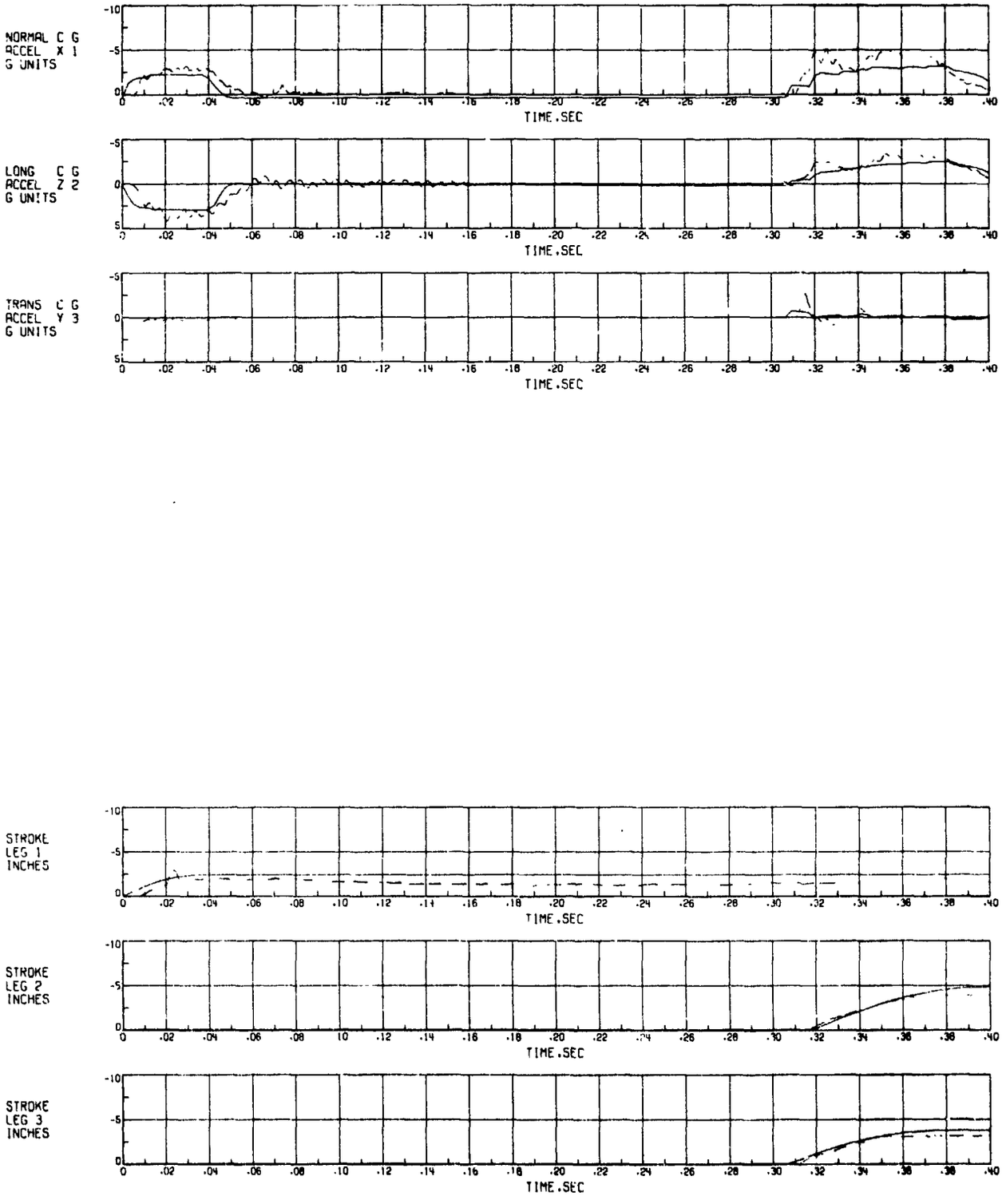


Figure 29.- Accelerations and Strokes versus Time - Drop Case 10.

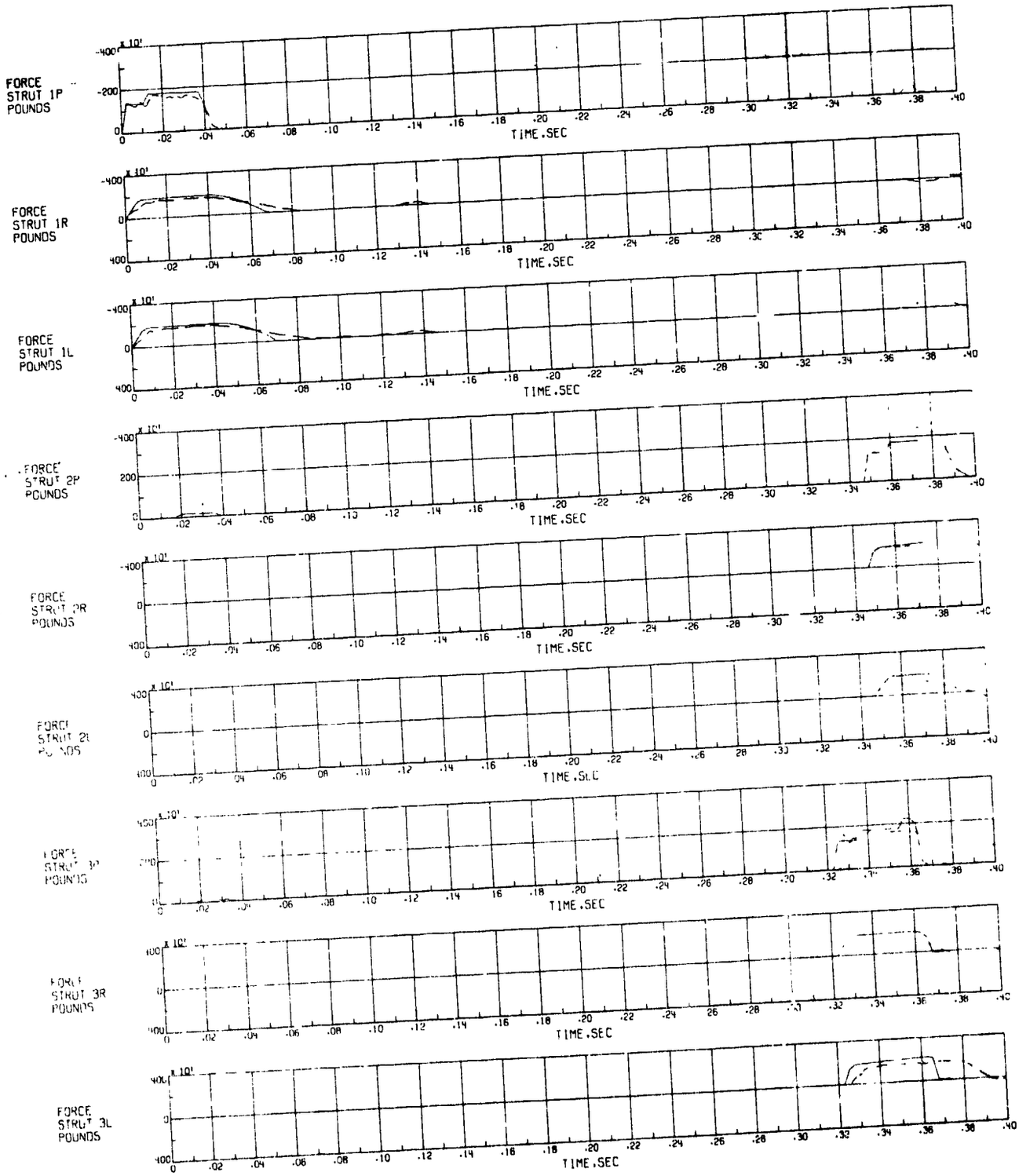


Figure 30.- Strut Forces versus Time - Drop Case 11.

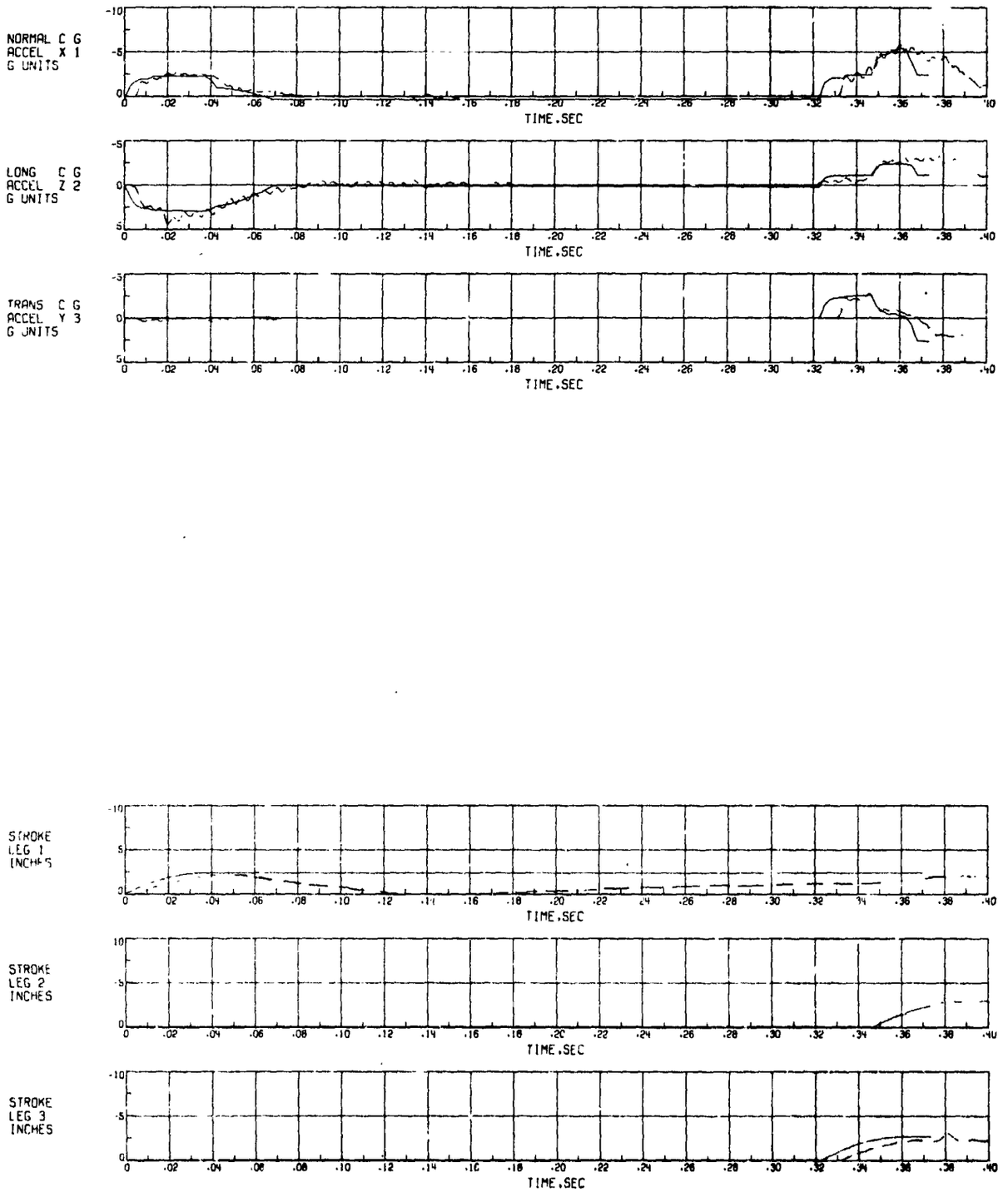


Figure 31.- Accelerations and Strokes versus Time - Drop Case 11.

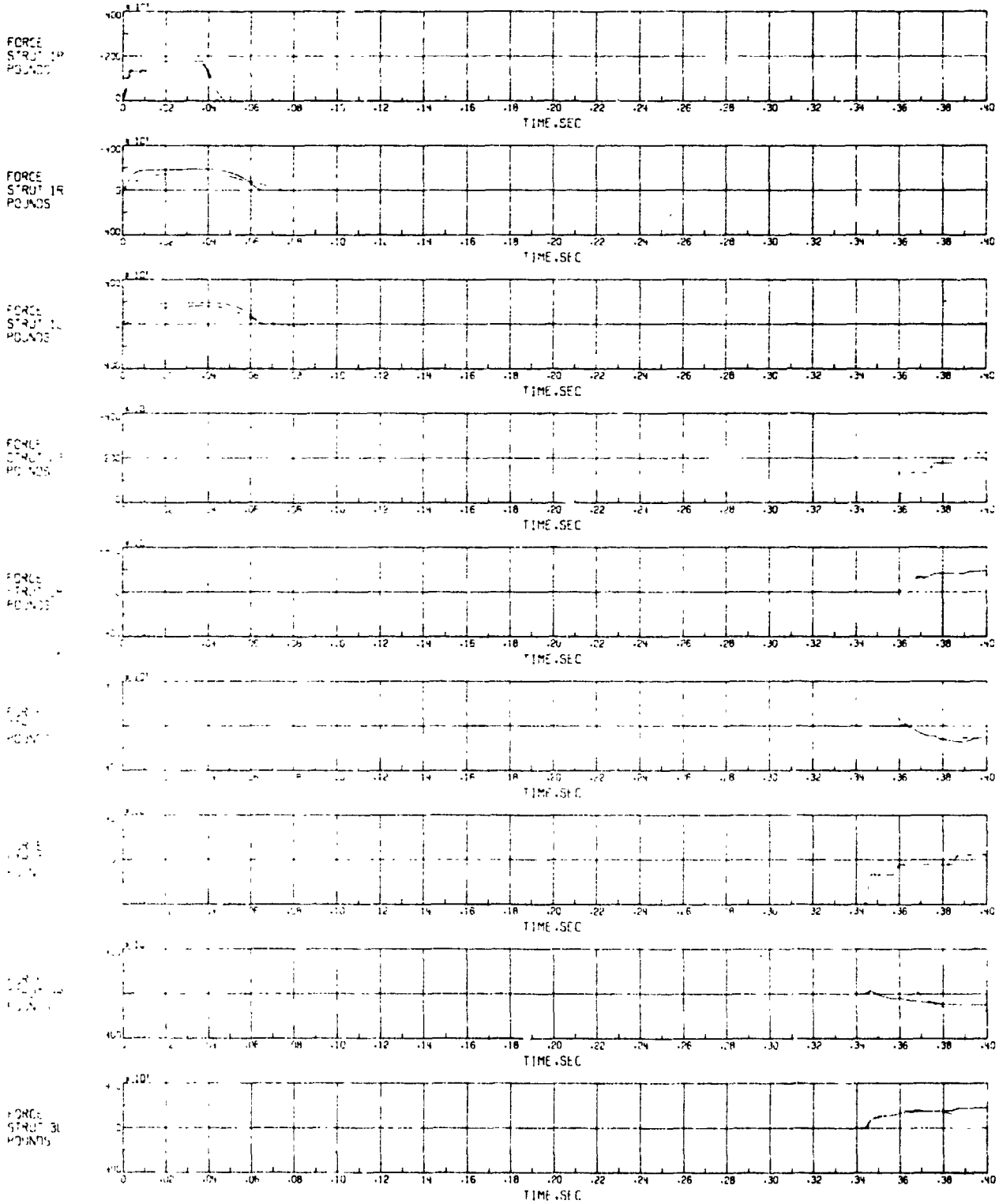


Figure 32.- Strut Forces versus Time - Drop Case 12.

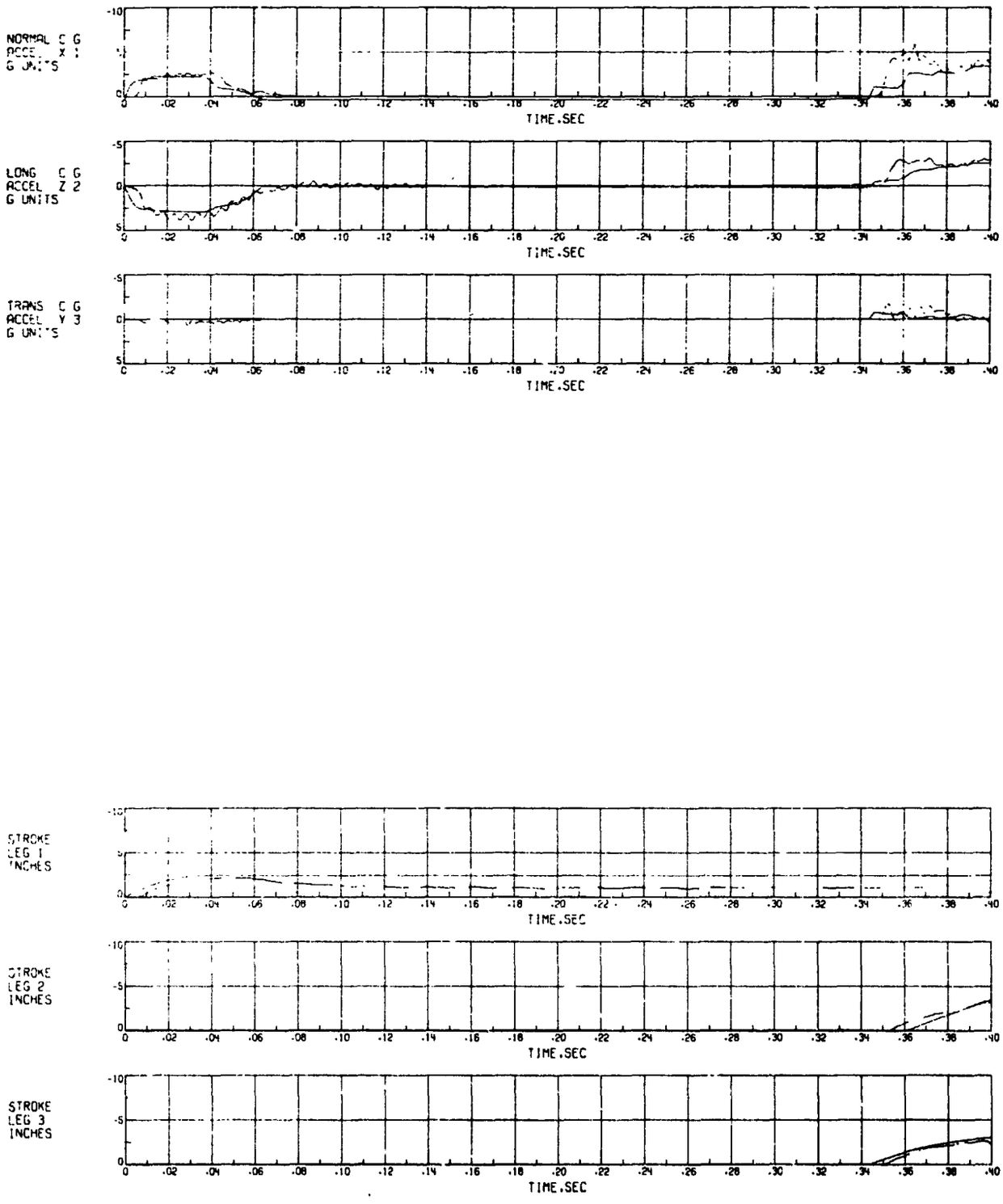


Figure 33.- Accelerations and Strokes versus Time - Drop Case 12.

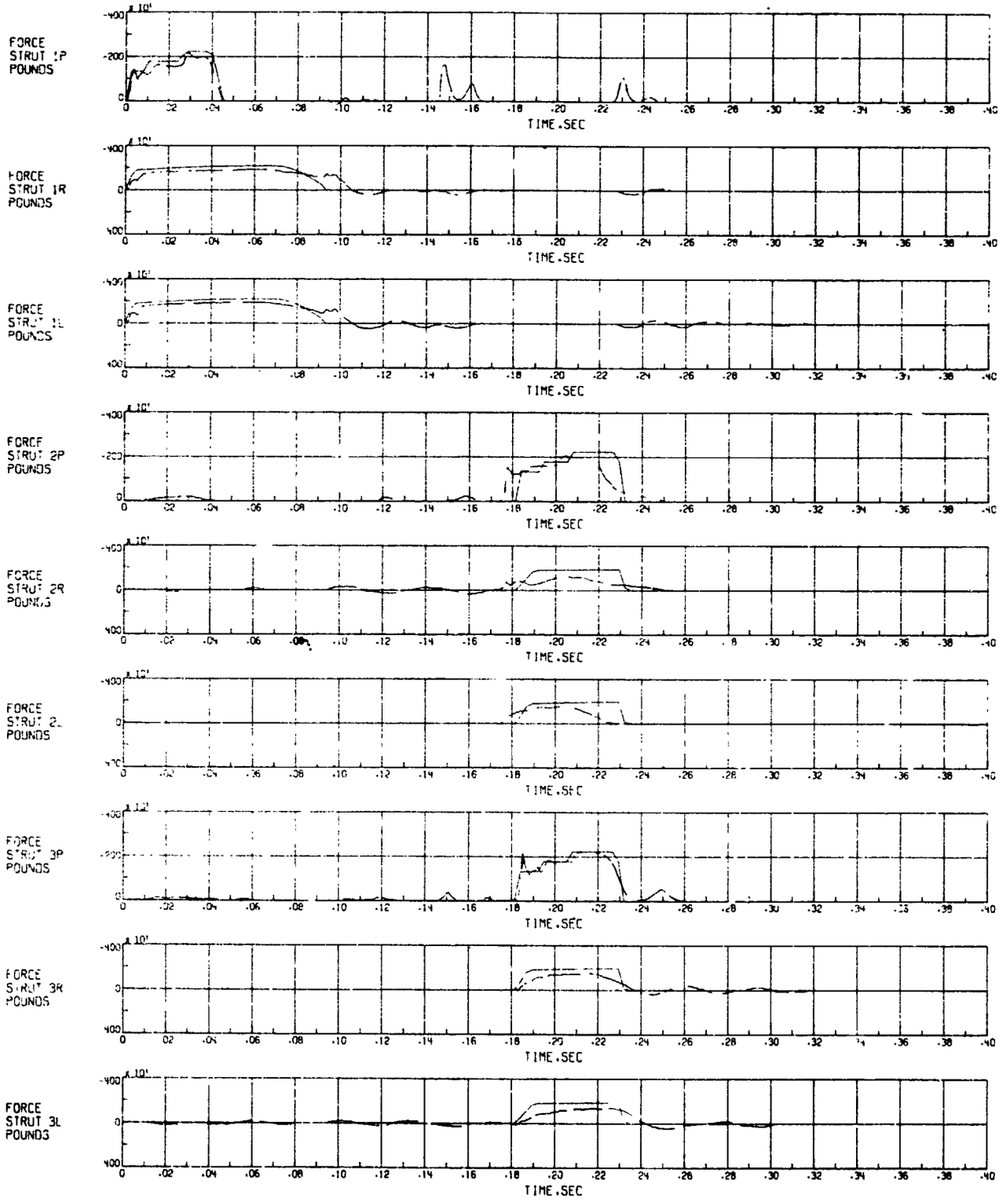


Figure 34.- Strut Forces versus Time - Drop Case 14.

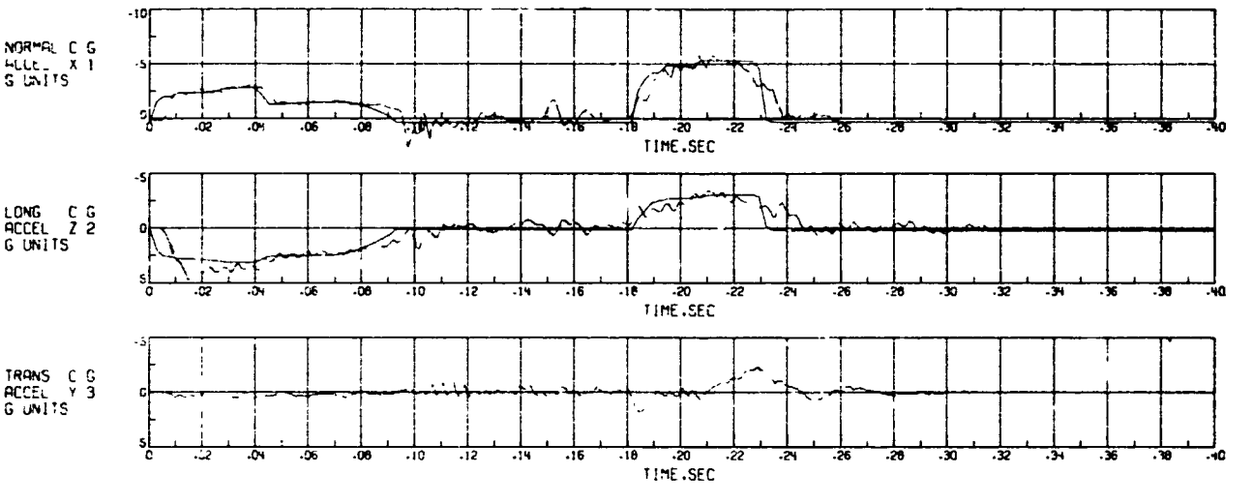


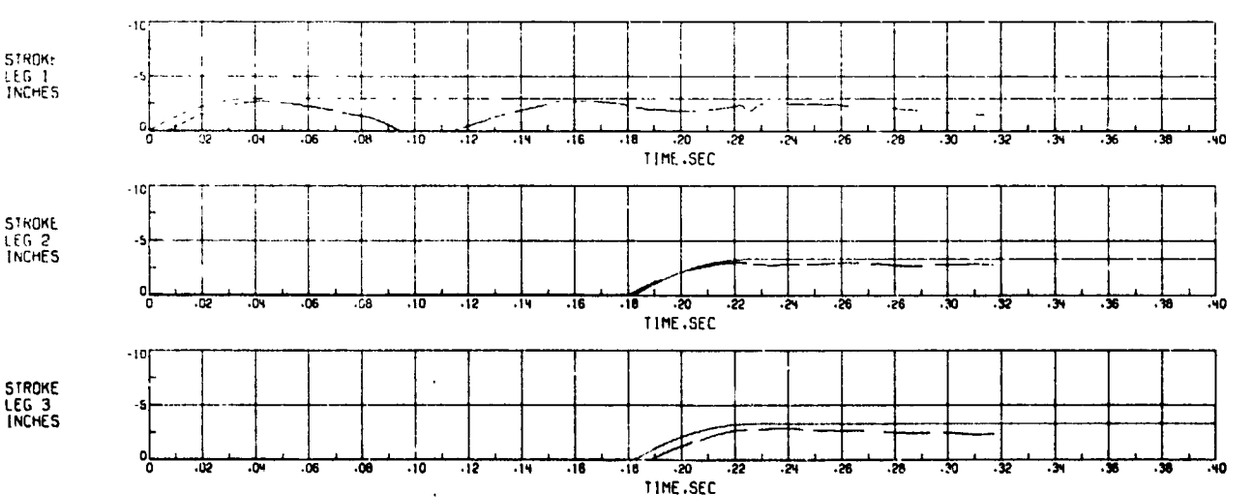


Figure 35.- Accelerations and Strokes versus Time - Drop Case 14.

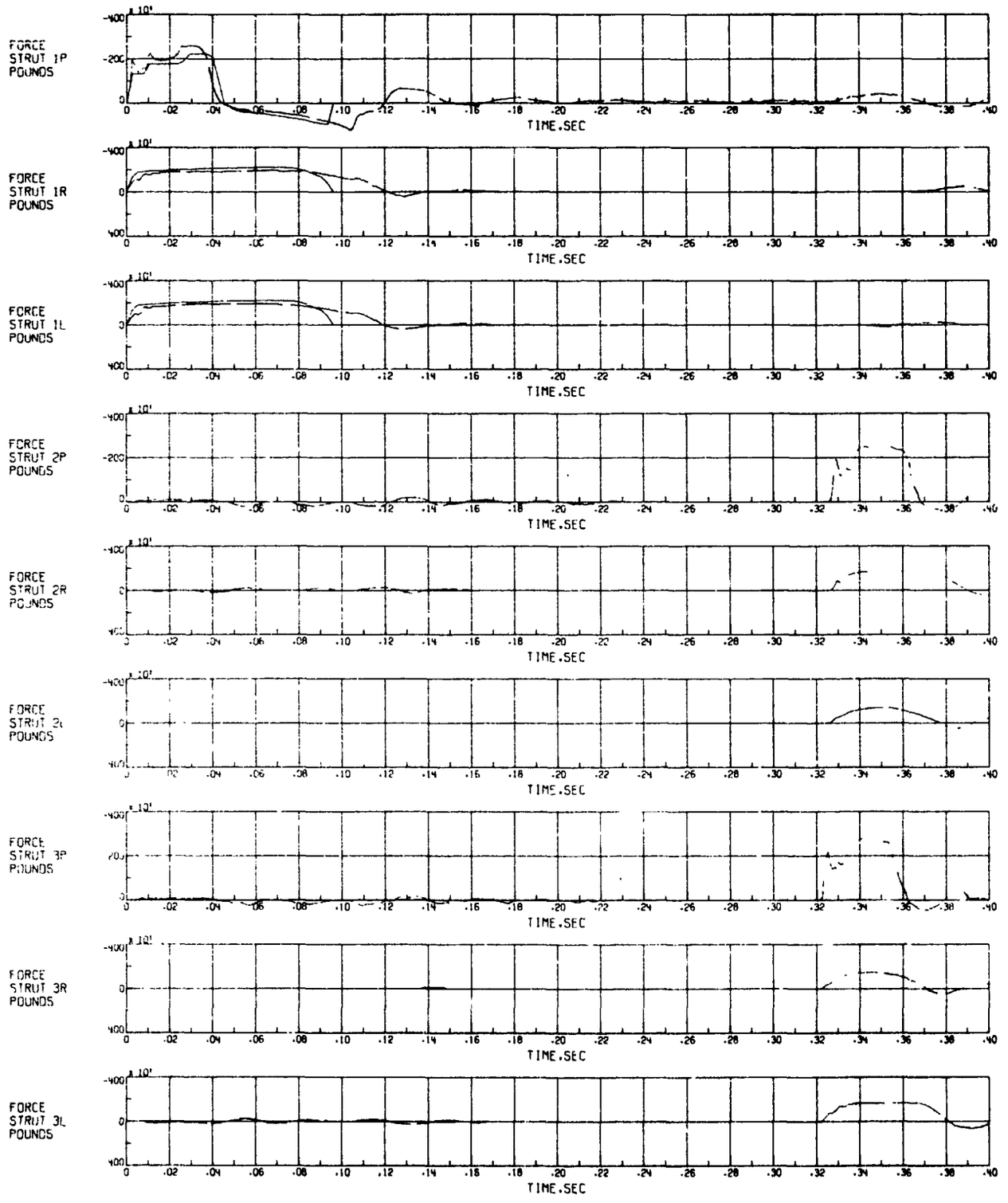


Figure 36.- Strut Forces versus Time - Drop Case 16.

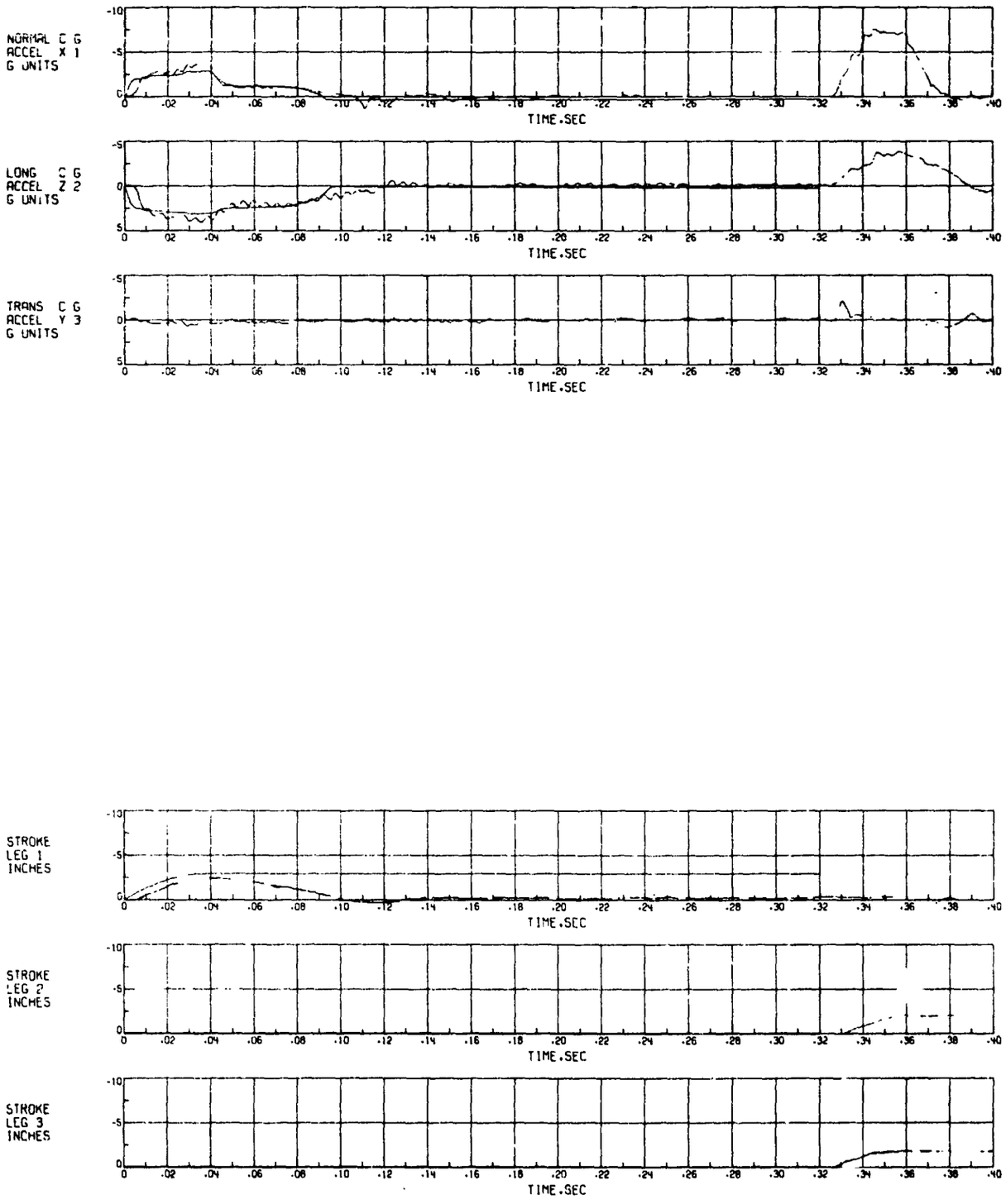


Figure 37.- Accelerations and Strokes versus Time - Drop Case 16.

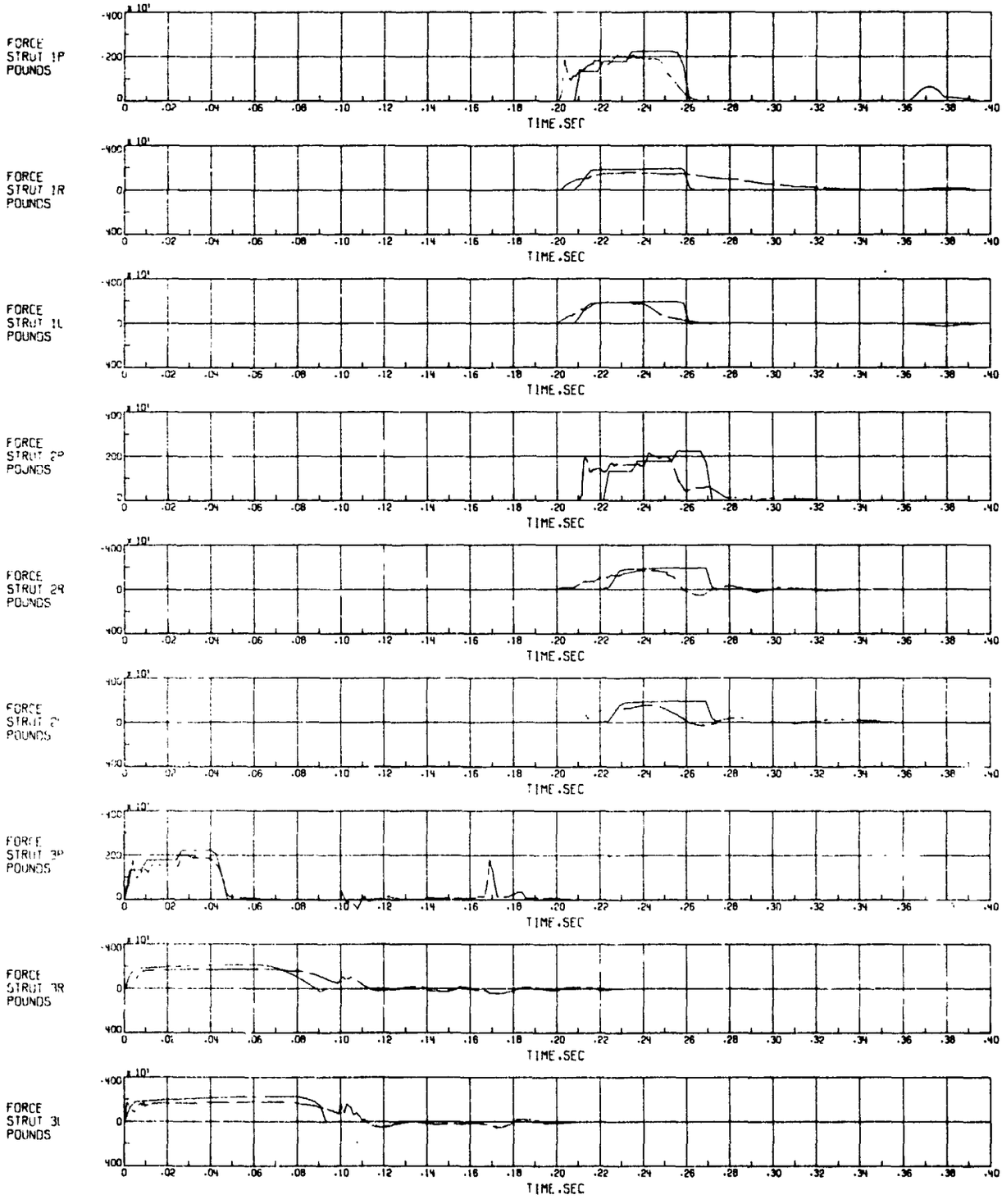


Figure 38.- Strut Forces versus Time - Drop Case 18.

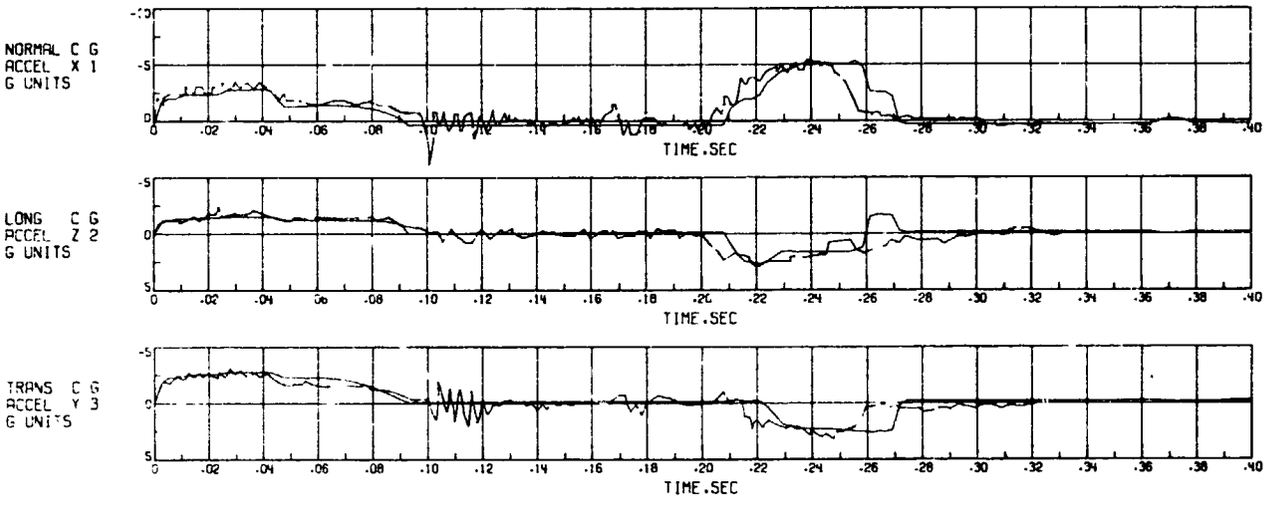


ORIGINAL PAGE IS
OF POOR QUALITY

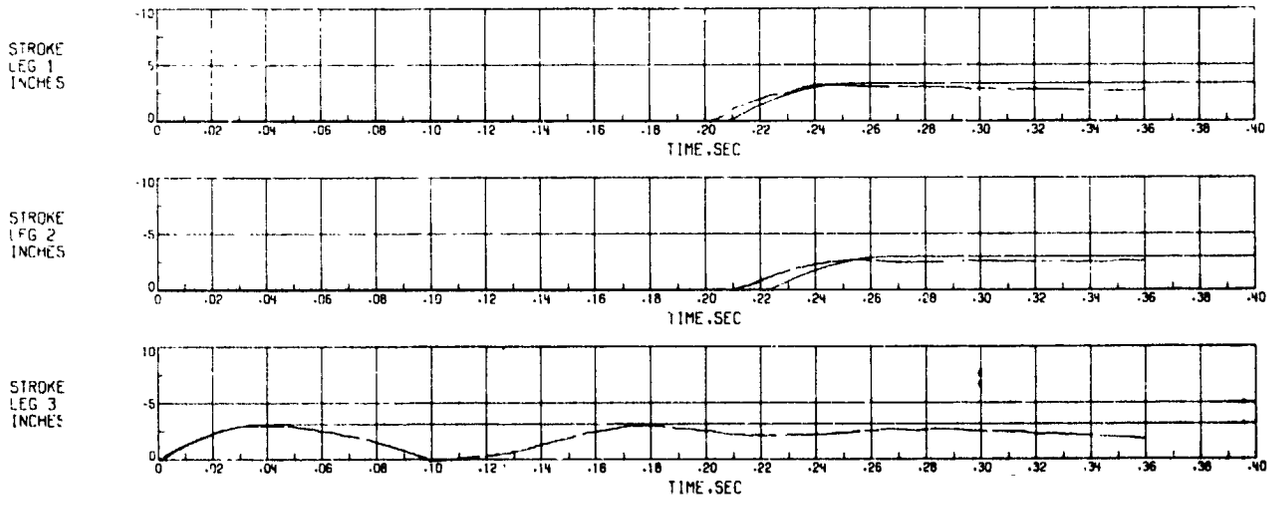


Figure 39.- Accelerations and Strokes versus Time - Drop Case 18.